

Photocopy and Use Authorization

In presenting this thesis in partial fulfillment of the requirements for an advanced degree at Idaho State University, I agree that the Library shall make it freely available for inspection. I further state that permission for extensive copying of my thesis for scholarly purposes may be granted by the Dean of the Graduate School, Dean of my academic division, or by the University Librarian. It is understood that any copying or publication of this thesis for financial gain shall not be allowed without my written permission.

Signature _____

Date _____

Cesium-137 Lake Sediment Depth Profiles and Inventories

in Idaho's Sawtooth Wilderness

by

Benjamin Bishop

A thesis

submitted in partial fulfillment

of the requirements for the degree of

Master of Science in the Department of Nuclear Engineering and Health Physics

Idaho State University

Spring 2018

Committee Approval

To the Graduate Faculty:

The members of the committee appointed to examine the thesis of Benjamin T. Bishop find it satisfactory and recommend that it be accepted.

Dr. Richard Brey,
Major Advisor

Dr. Thomas Gesell,
Committee Member

Dr. DeWayne Derryberry,
Graduate Faculty Representative

Dedication

The contents of this study are dedicated to the employees of the Sawtooth National Forest and the Sawtooth National Recreation Area. Jill Allgood, Heidie Torrealday, Christine Melvin, Kirk Flannigan, and Arthur Fisher all had a hand in making this the first research project to quantify ^{137}Cs sediment concentrations in Idaho's alpine lakes. May the contents be both informative and useful in your future endeavors.

Table of Contents

List of Figures.....	vii
List of Tables.....	ix
List of Abbreviations.....	x
Abstract.....	xi
Chapter I: Introduction.....	1
General Introduction to the Study.....	1
Statement of Research Purpose.....	3
Specific Research Objectives.....	3
Hypothesis.....	3
Chapter II: Literature Review.....	5
Introduction to the Sawtooth National Forest.....	5
Introduction to the Literature.....	6
Review of Relevant Literature.....	7
Overview of High Purity Germanium Detectors.....	10
Detection Limits.....	17
Chapter III: Methods and Materials.....	20
Research Approach.....	20
Sample Collection.....	22
Sample Analysis.....	25
Quality Assurance.....	26
Chapter IV: Results.....	28
Cesium-137 Depth Profiles.....	28

Chapter V: Summary and Conclusions.....	35
Discussion of Research Findings.....	35
Future Research Possibilities.....	37
References.....	40
Appendix A: List of Materials.....	45
Appendix B: Sample Maps.....	47
Appendix C: MAPEP Data.....	49
Appendix D: Sawtooth National Recreation Area Project Approval.....	50
Appendix E: High Purity Germanium Detection Specifications.....	51
Appendix F: ¹³⁷ Cs Concentration Numerical Sample Results.....	53

List of Figures

Figure 1: Borders of the Sawtooth Wilderness.....	5
Figure 2: ^{137}Cs Fallout Recorded Within the 40°N to 50°N Latitude Band.....	7
Figure 3: ^{137}Cs Activity vs. Depth for Select Adirondack Lakes.....	8
Figure 4: Observed ^{137}Cs Quantities in 1-cm Sediment Segments from Pine Valley Reservoir...	10
Figure 5: ^{137}Cs Radionuclide Transformation Data.....	11
Figure 6: Band Structure for Electron Energies in Insulators and Semiconductors.....	11
Figure 7: Acceptor Impurity Occupying a Spot in a Semiconductor Crystal.....	12
Figure 8: Donor Impurity Occupying a Spot in a Semiconductor Crystal.....	12
Figure 9: Reverse Bias in an N-P Junction Causes a Depletion Region.....	13
Figure 10: Comparison of HPGe and Scintillator Resolutions.....	14
Figure 11: Diagram Showing the Location of a HPGe Detector Within its Vacuum Capsule.....	14
Figure 12: Block Diagram of a HPGe Detector.....	15
Figure 13: The Common Basis for Setting L_C	17
Figure 14: The Common Basis for Setting L_D	18
Figure 15: Sampling Sites Within the Sawtooth Wilderness.....	21
Figure 16: Sample Preparation.....	24
Figure 17: Lake Alice ^{137}Cs Depth Profile.....	28
Figure 18: Bench Lake 1 ^{137}Cs Depth Profile.....	29
Figure 19: Hell Roaring Lake ^{137}Cs Depth Profile.....	30
Figure 20: Little Sawtooth Lake ^{137}Cs Depth Profile.....	31
Figure 21: Sedimentation Rate Charts.....	33
Figure 22: Deposition and Sedimentation Relationships to Elevation, Latitude and pH.....	34

Figure 23: Sawtooth National Forest Special Use Permit.....50

Figure 24: Detector 04 Specifications.....51

Figure 25: Detector 07 Specifications.....52

List of Tables

Table 1: ^{137}Cs Inventories in U.S. Lakes and Reservoirs in mCi km^{-2}	2
Table 2: Sampling Locations for ^{137}Cs in the Sawtooth Wilderness.....	21
Table 3: Summary of Research Findings.....	35
Table 4: Specifics of Alice Lake Sampling.....	47
Table 5: Specifics of Bench Lake 1 Sampling.....	47
Table 6: Specifics of Hell Roaring Lake Sampling.....	48
Table 7: Specifics of Little Sawtooth Lake Sampling.....	48
Table 8: Mixed Analyte Performance Evaluation Program Soil Source (8/1/2016).....	49
Table 9: Detector 04 Specifications.....	51
Table 10: Detector 07 Specifications.....	52
Table 11: ^{137}Cs Deposition Numerical Sample Results.....	53

List of Abbreviations

ADC	Analog to digital converter
AMS	Arts Machine Shop
BLR	Baseline restorer
BNC	Bayonet Neill-Concelman (cable)
EML	Environmental Measurements Laboratory
Ge(Li)	Germanium crystals doped with lithium ions (detector)
HPGe	High-purity germanium (detector)
LLD	Lower limit of detection
MAPEP	Mixed Analyte Performance Evaluation Program
MARSSIM	Multi-Agency Radiation Survey and Site Investigation Manual
MCA	Multichannel analyzer
MDA	Minimum detectable activity
MDC	Minimum detectable concentration
NaI(Th)	Sodium iodide crystal doped with thallium (detector)
NCR	Net count rate
NIM	Nuclear instrumentation module
NNDC	National Nuclear Data Center
PVC	Polyvinyl chloride
SHV	Safe for high voltage cable)
ULD	Upper limit of detection
USB	Universal serial bus (cable)

Abstract

Cesium-137 Lake Sediment Depth Profiles and Inventories in Idaho's Sawtooth Wilderness

Thesis Abstract--Idaho State University (2018)

A total of 68 sediment cores from four freshwater alpine lakes in Idaho's Sawtooth Wilderness were collected during the summer of 2017. The objectives of the study were to determine depth distributions of ^{137}Cs in the cores using gamma spectrometry and estimate the sedimentation rates of the lakes from the identified geochronological peaks linked to nuclear fallout. Cesium-137 radioactivity above background was detected in all studied lakes. The maximum ^{137}Cs concentrations measured in each lake's sediment ranged from 74.0 ± 6.09 to 255.3 ± 7.48 Bq kg^{-1} . Relationships between total ^{137}Cs deposition and elevation, latitude, and pH were tested and found to be nonexistent, but lake flushing and geological location are suggested to be primary factors. Three of the lakes had ^{137}Cs sediment depth distributions that resembled the deposition pattern of weapons testing as a function of time. Mean sedimentation rate estimates ranged from 0.08 ± 0.29 to 0.12 ± 0.05 cm y^{-1} and decreased with increasing altitude.

Chapter I: Introduction

General Introduction to the Study

The fallout from aboveground nuclear weapons tests deposited ^{137}Cs in soils worldwide. As such, ^{137}Cs remains one of the most environmentally ubiquitous radionuclides due to its global distribution on earth's surface and its persistent recycling in the biosphere. The fallout deposition provides the unique opportunity to study the scale and uniformity of radioactive contamination from weapons testing. Studies of ^{137}Cs have been widely used over the past decades as an indicator of radioactive contamination from fission products. The history of ^{137}Cs release into the atmosphere is well documented between the 40° and 50° latitude bands for the period of 1951 through 1985 (EML 1977; Heit and Miller 1987). A number of investigators have used ^{137}Cs to determine the chronologies of pollutant deposition into the sediments of a variety of aquatic ecosystems (Table 1) (Robbins and Edgington 1975; Pennington et al. 1976; Galloway and Likens 1979; Durham and Joshi 1980; Heit et al. 1980, Jaakkola et al. 1983).

Table 1. ^{137}Cs Inventories in U.S. Lakes and Reservoirs in mCi km^{-2} (Heit and Miller 1987)

Lake/Reservoir ^b	Location	Sediment inventory	Soil inventory	Ratio (%) ¹
Hinkley ^c	Grant, NY	335	98 ± 8	342
Great Sacadaga ^c	Northville, NY	251	98 ± 8	256
Stillwater ^c	Town of Webb, NY	151	98 ± 8	154
Cranberry ^c	Clifton, NY	91	98 ± 8	93
Other U.S. lakes and reservoirs ^a				
Upper enterprise ^d	Enterprise, UT	750	101	750
Nottely ^e	Murphy, NC	687	[120]	570
Lake Mead ^f	Overton Beach, NV	>583		
Deer Creek ^g	Heber City, UT	469	128	370
Echo ^g	Coalville, UT	361	(79)	(500)
Hansen ^h	Los Angeles, CA	>432		
Standley ¹	Jefferson County, CO	319	85-110	330
Grand ^g	Grand Lake, CO	260	82-98	300
Chatuge ^e	Murphy, NC	235	[120]	200
Santeetlah ^e	Robbinsville, NC	209	[120]	170
Cayuga ⁱ	Ithaca, NY	183	97	190
Blue Ridge ^e	Blue Ridge, GA	176	[120]	150
Gull Pond ^j	Cape Cod, MA	142	97	146
Utah Lake ^k	Provo, UT	110	118	93

^a All sites sampled were analyzed by EML

^b Major impoundments in the Adirondacks (basin > 10km²)

^c Heit (1987) ^d Krey et al. (1980) ^e Miller and Heit (1986)

^f Lake Mead ^{137}Cs inventory for 0-56 cm only (^{137}Cs was detected at bottom of core)

^g Hardy (EML, Personal communication, 1983)

^h Hansen reservoir ^{137}Cs inventory for 0 to 55 cm only (^{137}Cs was detected at bottom of core)

ⁱ Hardy (1980) ^j Heit et al. (1986) ^k Krey and Beck (1981)

¹ Ratio = [^{137}Cs inventory in sediment/ ^{137}Cs inventory in undisturbed soil] x 100%

Note:

[] Estimated ^{137}Cs soil inventories based upon ^{90}Sr deposition (Larsen 1985)

() Suspect soil inventory for Coalville, UT due to flooding

Information about ^{137}Cs deposition has been used to verify the success of remediation efforts in soil monitoring programs at nuclear power facilities within the United States. These programs typically compare remediated sites to uncontaminated background sites to demonstrate that no unacceptable levels of contamination remain. Many states have established background levels in the soil and sediment (Ulsh et al. 2000). However, background levels in Idaho's lakes within the Sawtooth Wilderness have not been measured. By examining both ^{137}Cs activity concentration and activity deposition values in the sediments of high-altitude sites, a background database can

be established for Idaho. Additionally, it can be determined whether there is any difference in variability between the measured sites.

Statement of Research Purpose

The aim of this study was to determine depth distributions of ^{137}Cs (Bq kg^{-1}) in sediment from several alpine freshwater lakes within Idaho's Sawtooth Wilderness. The data collected will provide a depth profile of the cesium, showing the pattern of fallout distribution in Idaho from aboveground nuclear weapons testing in the 1950s and 1960s. The research will add to the database of ^{137}Cs deposition in high-altitude lakes within the United States, provide information on the spatial distribution of ^{137}Cs in the Sawtooth Wilderness, and enhance the knowledge about present ^{137}Cs activity concentrations in Idaho. Furthermore, the data would establish baseline fission product backgrounds for some alpine lakes in Idaho, creating a comparative database in the event of any future nuclear releases.

Specific Research Objectives

The specific research objectives of this study were to:

- 1) Determine depth distributions of ^{137}Cs in sediment cores from several alpine freshwater lakes.
- 2) Use gamma spectrometry to detect ^{137}Cs peaks correlating to nuclear testing fallout.
- 3) Estimate the sedimentation rates of the alpine lakes tested from the detected ^{137}Cs peaks.

Hypothesis

The hypothesis is based on whether ^{137}Cs fallout activity can be detected within the Sawtooth Wilderness.

Null hypothesis (H_0): The environmental samples will not contain any activity above background as measured by the 661.6-keV gamma emission from the decay of $^{137\text{m}}\text{Ba}$.

Alternate hypothesis (H_1): The samples will contain quantifiable activity above background as measured by the 661.6-keV gamma emission from the decay of $^{137\text{m}}\text{Ba}$.

Decision rule: Reject the null hypothesis if $z > 1.645$.

Chapter II: Review of Literature

Introduction to the Sawtooth National Forest

The Sawtooth National Forest (Figure 1) was created under proclamation of President Theodore Roosevelt on 29 May, 1905 (Ewert and Sara 2000). Public Law 22-400, passed in 1972, established the Sawtooth National Recreation Area. At that time, the 217,088 acres of the Sawtooth Wilderness became part of the National Wilderness Preservation System (Osborn 1979). The Sawtooth Wilderness encompasses the Sawtooth Mountains. The boundaries include the watershed of the Snake River, which is a tributary of the Columbia River that flows into the Pacific Ocean. There are over a thousand lakes in the wilderness. Nearly all are the result of glaciation (U.S. Forest Service 1998).



Fig. 1. Borders of the Sawtooth Wilderness (U.S. Forest Service 1998)

Introduction to the Literature

Most investigations of cesium in soils have been conducted at low-to-mid-altitude sites. However, deposition and transport mechanisms at high-altitude sites differ from those prevalent at lower altitudes. Most fallout is removed from the atmosphere and transferred to soil via snowfall events at high altitudes. Cesium-137 and other atmospherically transported pollutants deposited on the snow and ice are released into the surface water during periods of thaw, which usually occurs during April and May (Heit and Miller 1987; Ulsh et al. 2000). It is estimated that the transported pollutants are not flushed from the lakes prior to being deposited in the sediment during these periods due to the undisturbed nature of the alpine lakes within the Sawtooth Wilderness. Scavenging by rainfall events and dry deposition are the primary mechanisms of atmosphere to soil transfer at lower altitudes. Snow is more effective at scavenging the atmosphere than rain (Sparmacher et al. 1993; Nicholson et al. 1991). Fallout deposition on soils is strongly absorbed, and ^{137}Cs is firmly bound to clay mineral particles in riverine and lake sediments (Comans et al. 1991; Robbins et al. 1992). Cesium-137 within aquatic environments is taken up by the organisms inhabiting them and transferred through the food chain. Upon the organism's death, the ^{137}Cs is concentrated into the sediment (Saxén and Ilus 2008; Fesenko et al. 2011). The presence of a ^{137}Cs fallout pattern within a sediment core obtained from an undisturbed lake bed is anticipated to allow for an accurate reconstruction of the chronology of the weapons testing time period. Large peaks are not expected to be seen before 1951 when major weapons testing began in the continental United States. Two distinguishable ^{137}Cs peaks related to weapons testing are likely to be seen in sediment cores (Figure 2). The first anticipated peak, deepest in the sediment, if observed is likely to represent the period from 1958 to 1959. The largest peak is indicative of weapons testing in 1963. The

^{137}Cs levels after 1963 declined rapidly as a result of signing the Nuclear Test Ban Treaty (Heit and Miller 1987).

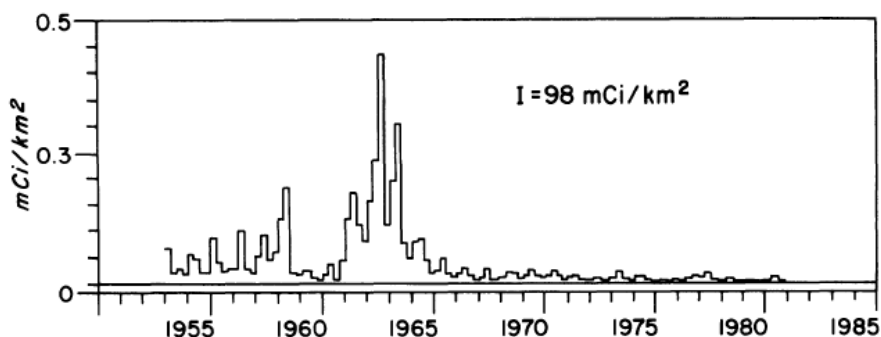


Fig 2. ^{137}Cs Fallout Recorded Within the 40°N to 50°N Latitude Band (Heit and Miller 1987)

The use of ^{137}Cs as a sedimentation indicator is typically effective because it strongly adheres to clay minerals and is long-lived. Sediments generally contain greater than 99% of a lake's total ^{137}Cs inventory due to this feature (Whicker et al. 1990). Detailed fallout history depth profiles of lakes may be obtained from sediment cores from alpine lakes as the ^{137}Cs concentrates in the sediment layers are not easily disturbed. The fallout levels measured are specific to each region, varying with climatic conditions, land formations, latitude, distance from detonation, and type of detonation device. In the continental United States, the greatest amount of radioactive fallout was deposited in 1964, and the second largest deposition was in 1959 (Whicker et al. 1994). Using these dates, it is hypothesized that gamma spectrometry will show clear maxima of ^{137}Cs corresponding to these years, and mean sedimentation rates of the lakes may be estimated by dividing the depth of the corresponding peaks by the associated time lapse.

Review of Relevant Literature

Four notable studies measuring ^{137}Cs depth profiles within lakes and reservoirs have been conducted within the United States since 1987. In that year, Heit and Miller within the Department of Energy studied nine lakes between elevations of 500 to 700 m in the New York State Adirondack Preserve in addition to Mirror Lake within the White Mountain region of New

Hampshire. A 21-cm diameter soil corer took a single sample down to 90 cm at the deepest part of each lake. Each 1-cm increment was measured for 100 minutes within a Teflon-lined aluminum can using a high-resolution germanium detector and a 4,000-channel analyzer. None of the Adirondack Lakes had ^{137}Cs depth distributions that resembled the deposition pattern of weapons testing as a function of time. Rather, all lakes had significantly lower ^{137}Cs inventories than expected and showed a single ^{137}Cs peak (Figure 3), indicating mechanisms of mixing or resuspension of the sediments had occurred (Heit and Miller 1987).

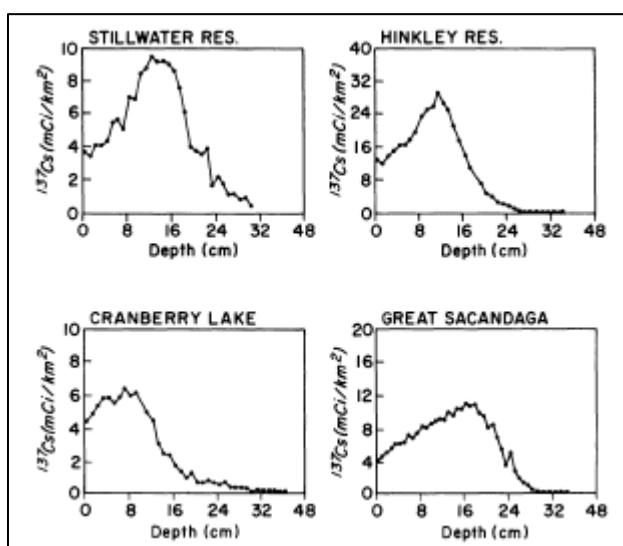


Fig 3. ^{137}Cs Activity vs. Depth for Select Adirondack Lakes (Heit and Miller 1987)

The results of this study led the Department of Energy to conclude that the lack of binding clay-like minerals allowed the ^{137}Cs to mobilize from lake sediment to the lake outlets through diffusion and redeposit downstream. Additionally, substantial currents during spring thaw flushed ^{137}Cs deposited on the ice from the lakes prior to sediment deposition. This effect was less common in large bodies of water with fast rates of sedimentation (Heit and Miller 1987).

The largest study conducted occurred between 1992 and 2001. It was accomplished by the U.S. Geological Survey. The research analyzed samples from 45 reservoirs and 11 lakes from a variety of elevations within eighteen states. The aim of the study was to determine the impact of

urbanization on water quality. Sampling methodology varied between each water body, being completed with gravity, push, piston, and box corers. However, all core segments were stored and analyzed by a high-purity germanium spectrometer within polypropylene jars. An analysis of the influence of environmental factors on the quality of the cores indicated that the most important factor was the sediment mass accumulation rate. Water bodies having the clearest ^{137}Cs deposition relative to weapons testing had the largest sediment mass accumulation rates, while there was no distinction between lakes and reservoirs. The ^{137}Cs depth distributions in these cores typically had a single peak, which was assigned a date of 1964 (Van Metre et al. 2004). There was little correlation between samples regarding the measured activity and the depth of the observed peak.

Fifteen impoundments in Utah, two in Oregon, and one in Colorado were investigated by members of Los Alamos National Laboratory and Colorado State University in 1992. The bodies of water ranged from 1,615 to 3,109 m in elevation. Three to four samples were taken at each lake to a depth of 2 m using polyvinyl chloride (PVC) gravity corers with a 3-cm diameter. Cores were analyzed by Ge(Li) and NaI(Tl) detectors in 1-cm segments after the multiple samples were homogenized and dried. The cores from these bodies of water, such as Pine Valley Reservoir, had ^{137}Cs depth distributions (Figure 4) expected from the deposition pattern of weapons testing (Whicker et al. 1994).

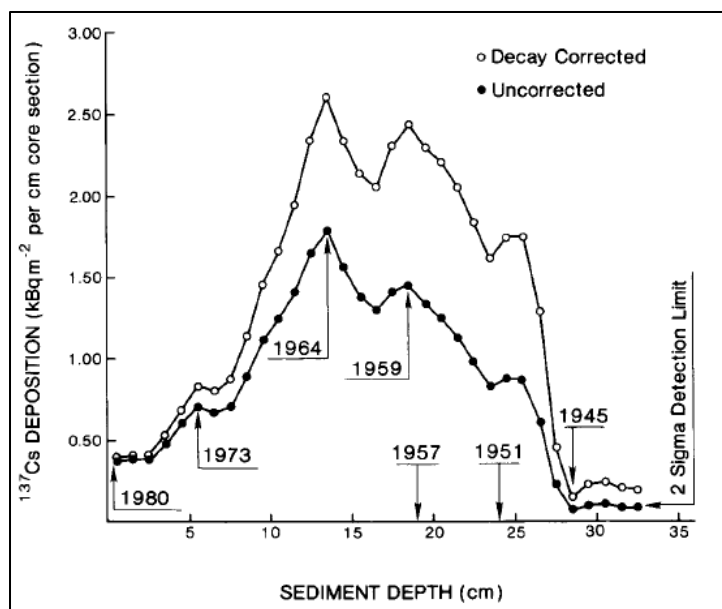


Fig 4. Observed ^{137}Cs Quantities in 1-cm Sediment Segments from Pine Valley Reservoir (Whicker et al. 1994)

The study also determined that total ^{137}Cs deposition decreased linearly with increasing altitude. This was a result of the watershed area contributing to drainage that was thought to increase at lower elevations, increasing runoff and erosion and causing subsequent sedimentation in lower water bodies (Whicker et al. 1994). This supported a hypothesis that total ^{137}Cs deposition in sediments was a result of both direct deposition into the lake body as well as deposition caused by soil erosion from the surrounding watershed (Krey et al. 1990).

Overview of High Purity Germanium Detectors

The radionuclide ^{137}Cs is solely created from anthropogenic activities and has a half-life of 30.08 years (NNDC 2017). Cesium-137 is a pure beta-emitter (Figure 5), but is most easily measured from the 661.6-keV gamma emission from its $^{137\text{m}}\text{Ba}$ daughter (Eisenbud and Gesell 1997). The daughter, having a half-life of 2.6 minutes, can be measured via gamma spectroscopy with a semiconductor detector (NNDC 2017).

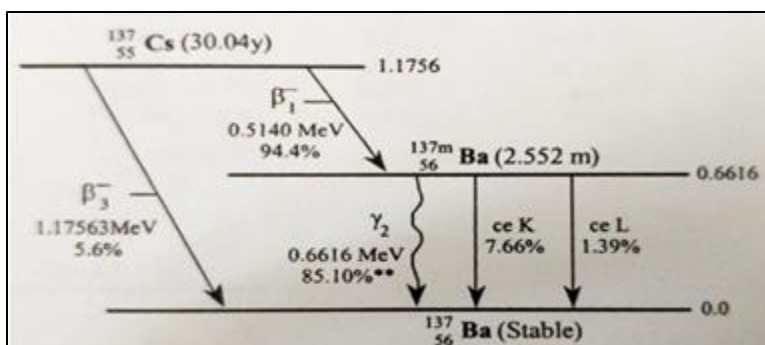


Fig 5. ^{137}Cs Radionuclide Transformation Data (Martin 2013b)

Outer shell electrons bound to a specific lattice within a crystalline material reside in the valence band. The conduction band consists of electrons free to move about the crystal. Electron energy flows from the valence band to the conduction band. Between the bands exists the energy gap. The size of the energy gap determines the conductivity properties of the crystal. An energy gap greater than 5 eV creates an insulator, while gaps in the range of 1 eV create semiconductors (Figure 6). Germanium serves as a good semiconductor due to the small energy gap between its conduction and valence bands (Poudel 2015a).

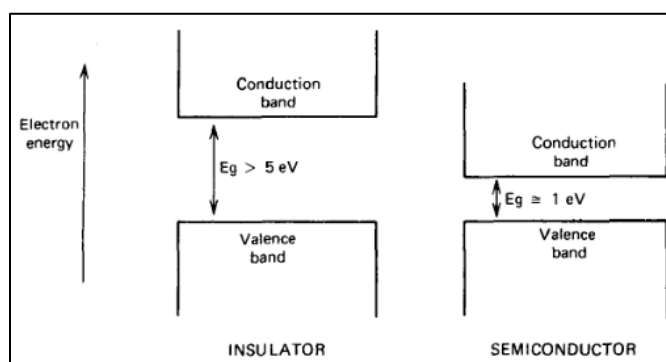


Fig 6. Band Structure for Electron Energies in Insulators and Semiconductors (Knoll 2010b)

The germanium used in semiconductor materials must be highly purified. Purification is accomplished through zone refining in which molten zones are passed through the crystal in a single direction to remove impurities. After zone refining the resulting crystals will be either a p-type or n-type crystal because it is not possible to grow a semiconductor crystal that is

absolutely free of impurities. The p-type crystal is a trivalent crystal, meaning it can accept an electron to form a covalent bond (Figure 7).

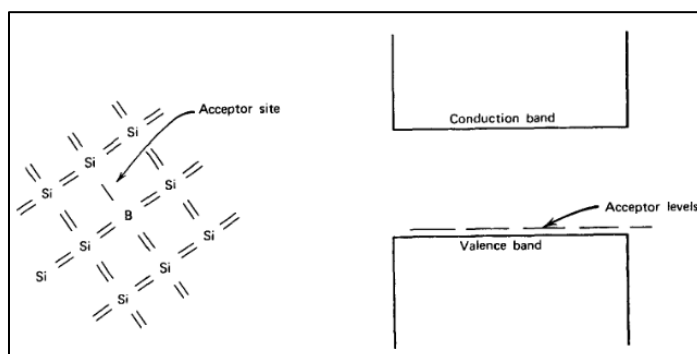


Fig 7. Acceptor Impurity Occupying a Spot in a Semiconductor Crystal (Knoll 2010b)

N-type crystals are pentavalent crystals, meaning they have an additional electron that is free to bond covalently with other atoms (Figure 8). These pentavalent atoms are referred to as donor impurities.

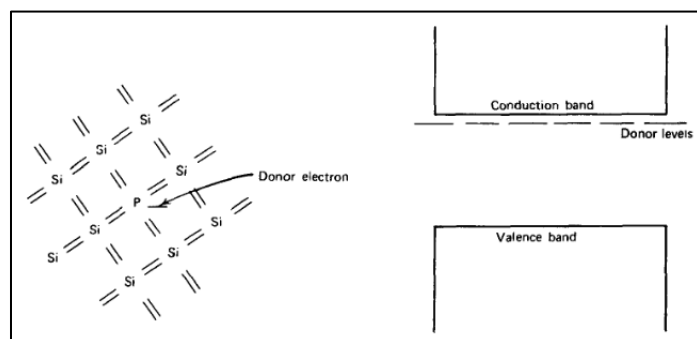


Fig 8. Donor Impurity Occupying a Spot in a Semiconductor Crystal (Knoll 2010b)

Acceptor or donor impurities may be compensated for by adding the opposite impurity during crystal formation. A p-type or n-type crystal bias will always occur since exact compensation cannot be achieved. Detectors made from ultrapure germanium are called high purity germanium (HPGe) detectors (Konzen 2017).

Semiconductor material can be arranged within an electrical circuit so current may only flow in one direction. An n-type contact is formed by implanting a donor ion into the face of the crystal. A p-type face is made on the opposite side by attaching a metallic contact. An n-p

junction is therefore formed, within which exists an intrinsic region. The intrinsic region determines the size and efficiency of the detector. An n-p junction under a reverse bias will conduct very little current. The width between the two faces is the detector volume, which is known as the depletion region (Figure 9).

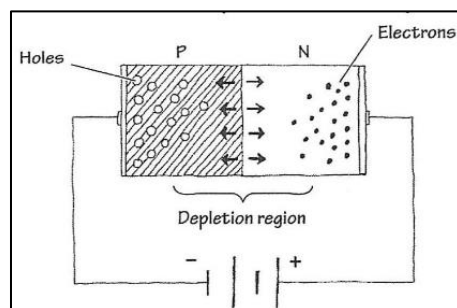


Fig 9. Reverse Bias in an N-P Junction Causes a Depletion Region (Konzen 2017)

Energy deposited into semiconducting material can excite electrons from filled valence bands to conduction bands. This results in a pair of conduction electrons and vacancies called holes. The number of electrons and hole pairs produced when radiation interacts with a semiconductor material is proportional to the energy deposited into the detector by the radiation (Konzen 2017; Poudel 2015a). The reverse bias voltage placed across the semiconductor causes the charge carriers to move towards their respective polarities as soon as they are developed in the depletion region. The charges collected on the electrodes are integrated by a preamplifier and converted to a voltage pulse (Martin 2013a; Konzen 2017). The incident energy required to produce a pulse within a semiconductor detector is around 3 eV; considerably less than that required to produce ionizations for a scintillation detector. A relatively high number of charge carriers is produced in a semiconductor detector for each photon absorbed. The statistical fluctuations of excited or ionized atoms are consequently less, causing very sharp pulses when used with a multichannel analyzer (MCA). This high resolution allows energies to be determined very accurately in a

semiconductor detector compared to a scintillation detector (Figure 10) (Poudel 2015a; Martin 2013a).

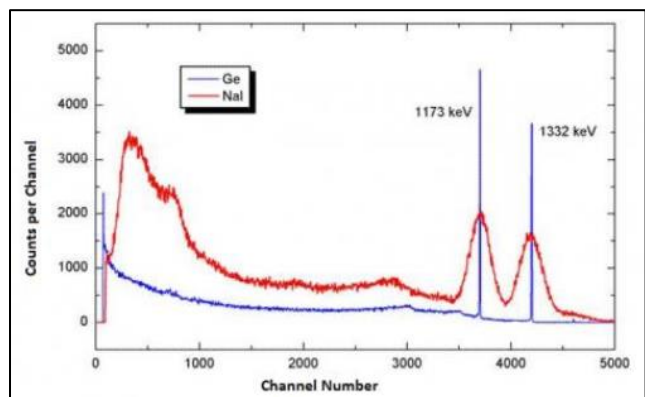


Fig 10. Comparison of HPGe and Scintillator Resolutions (Konzen 2017)

HPGe detectors must be cooled to reduce leakage current which contributes to background noise. The detector is therefore mounted in a cryostat. The crystal is mounted in a vacuum chamber within the cryostat, which is connected via a cold finger to a liquid nitrogen tank (Figure 11).

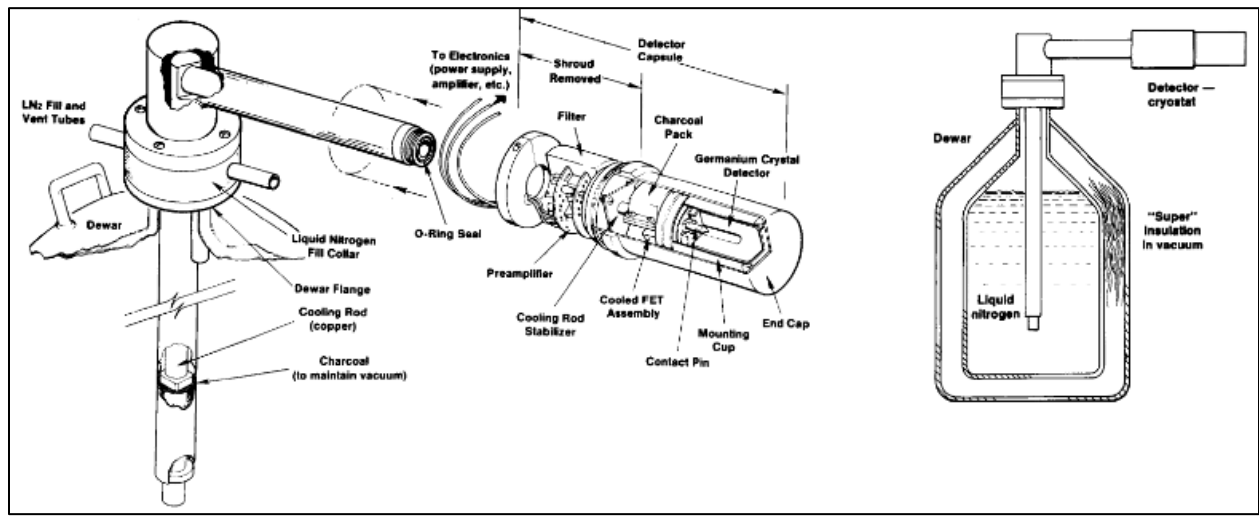


Fig 11. Diagram Showing the Location of a HPGe Detector Within its Vacuum Capsule (Konzen 2017)

A thin end window is located near the surface of the crystal to allow radiation entry. The thickness of the window determines the photon energy range the detector can measure. HPGe

detectors are commonly used for gamma-ray detection up to a few MeV and high-energy x-ray detection (Konzen 2017; Brey 2017).

Another instrument used in gamma spectroscopy is the MCA. An MCA is a device that can measure distributions of input signals consisting of pulses. There are two types of calibrations required for MCAs: energy and efficiency calibrations, though Full Width Half Max versus energy is also sometimes used. Energy calibration is used to assign photon energy to each channel on the MCA. A relationship can be developed in which the channel number for a given energy can be calculated, as shown in eqn 1, once an appropriate number of channels has been selected and the energy range of interest is known.

$$Channel_{\#} = \frac{(E_{source})(\#Channels_{desired})}{2 keV} \quad (1)$$

A linear set of data is obtained which correlates the channel number with the observed peak centroids of gamma ray emitters when completed with multiple sources. An unknown source could be identified through the regression line equation fit to the energy calibration data by correlating an observed peak on a channel number to the photon energy of the decaying radionuclide (Brey and Claver 2017; Poudel 2015a). A block diagram of the final setup of a HPGe connected to all components is shown in Figure 12.

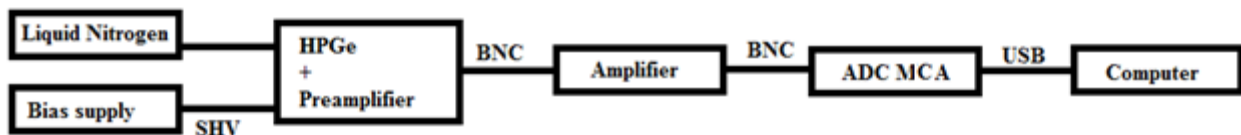


Fig 12. Block Diagram of a HPGe Detector

The efficiency calibration associates counting efficiency with photon energy. Efficiency is determined for each of the photon energies by measuring the area under each energy peak (Brey and Claver 2017). The measured value is the net count rate for the sample, which allows for the calculation of efficiency using eqn 2,

$$\varepsilon = \frac{NCR}{A \times Y} \quad (2)$$

where NCR is the net count rate, A is activity of the source, and Y is yield (Poudel 2015b). Eqn 2 can be corrected for decay by accounting for the number of half-lives ($\#T_{1/2}$) which have passed.

This results in eqn 3.

$$\varepsilon = \frac{NCR}{AYe^{\frac{-0.693 \times \#T_{1/2}}{\lambda}}} \quad (3)$$

A plot of photon efficiencies versus photon energy can be fitted to a function describing the detector response. The NCR provided by an unknown could then be correlated to the sample's efficiency. The activity concentration of the unknown ($Bq\ g^{-1}$), corrected for sample geometry, detector efficiency, yield, and radioactive decay to the date of collection, could be calculated by:

$$A = \frac{(C-B)e^{\lambda t}}{m\varepsilon Y} \quad (4)$$

where C is the total count rate (counts per second), B is the background count rate, λ is the decay constant (d^{-1}), t is the difference between the collection date and counting date (d), m is the mass of sample (g), ε is the detector efficiency, and Y is the yield for ^{137}Cs (Post 2011).

HPGe crystals are typically smaller than scintillation detector crystals, such as sodium iodide with thallium activators [NaI(Tl)]. The smaller size of the crystal and the lower atomic number of germanium (32) compared to sodium iodide (53) results in much lower counting efficiencies for HPGe detectors compared to NaI(Tl) crystals. The absolute efficiency of a HPGe detector compared to that of a NaI(Tl) detector is known as the relative efficiency. The absolute efficiency for a NaI(Tl) detector is 1.2×10^{-3} when measured on a $7.62\ cm^2$ crystal, 25 cm away from the 1,332 keV photon from ^{60}Co . The same setup is used to determine the absolute efficiency of the HPGe crystal as described in ANSI/IEEE No. 325-1996. The 1,332-keV photon is typically used because the gamma emission rate is accurately known.

$$\varepsilon_{relative} = \frac{\varepsilon_{HPGe,1,332\text{ keV } \gamma, 25\text{ cm}}}{\varepsilon_{NaI(Tl),1,332\text{ keV } \gamma, 25\text{ cm}}} \quad (5)$$

The equation for relative efficiency is given in eqn 5, where ε is efficiency (Konzen 2017; Poudel 2015a).

Detection Limits

Detection limits of a measuring device must be determined in order to conclude the activity levels of the sources with a degree of confidence. The limits are the critical level (L_C), the detection limit (L_D) and the minimum detectable activity (MDA). These limits help determine whether the activity measured by the detector is real or due to background. This is done through statistical analysis by approximating the rate of radioactive decay as a Poisson distribution.

The L_C is a set value the net counts (C_N) must surpass in order to conclude radioactivity is present above background. L_C is a flexible value which can be shifted to reflect the desired degree of confidence, though a value of 1.645 times the standard deviation (σ) of the data is most common (Figure 13). This equates to a 95% probability that samples with readings above the L_C actually contain some radioactivity. Therefore, the probability of concluding the presence of radioactive material when activity is absent (false positive error) is reduced to 5%.

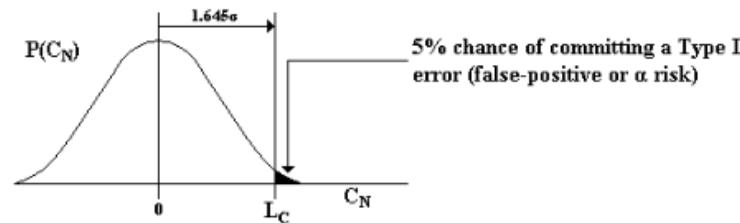


Fig. 13. The Common Basis for Setting L_C (Brey and Claver 2017; Currie 1968; Knoll 2000a).

When C_N is below L_C , it can be concluded that no radioactivity is present above background at the given confidence rate (Brey and Claver 2017; Currie 1968; Knoll 2000a). It can also be seen that:

$$L_C = 2.33\sqrt{Background} \quad (6)$$

for a 95% confidence interval, which estimates the standard error of the mean in a one-tail t-test determination (Poudel 2015c; Western Michigan University 2003).

It is possible to conclude no radioactivity is present when it is actually present (false negative error) when radioactivity is measured above background. This occurs when distributions for measured counts and background counts overlap (Figure 14).

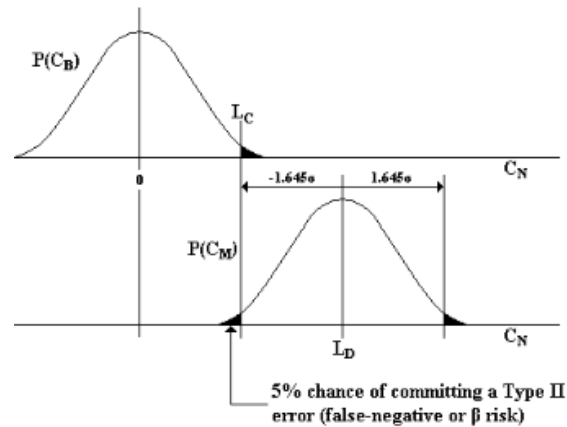


Fig. 14. The Common Basis for Setting L_D (Brey and Claver 2017; Currie 1968; Knoll 2000a).

The L_D is a minimum value which measured counts must exceed in order to minimize false negative errors. The conventionally accepted error rate is 5%. There is a 95% probability that a random sample will lie above the mean minus 1.645σ in a Gaussian distribution, where σ is the standard deviation. Fig. 4 shows that L_D must be set at 1.645σ of the L_D distribution greater than L_C (Brey and Claver 2017; Currie 1968; Knoll 2000a). L_D may also be calculated using one-tail t-test estimations by

$$L_D = 2.71 + 4.65\sqrt{Background} \quad (7)$$

for a 95% confidence interval (Poudel 2015c).

MDA is the smallest quantity of a radioisotope which can be detected with a given detector setup. It is based on statistical variation in detector counting in the region where the source would normally be detected. If the variation in counts is greater than the gross counts from the

radioisotope, the source will not be detected due to statistical insignificance (Berkeley University 2014). Eqn 8 is used to convert L_D to MDA,

$$MDA = \frac{L_D}{Y\varepsilon T} \quad (8)$$

where Y is yield per disintegration, ε is efficiency, and T is counting time for the sample (Brey and Claver 2017; Currie 1968; Knoll 2000a). Dividing the MDA by sample volume results in the Minimum Detectable Concentration (MDC).

Chapter III: Methods and Materials

Research Approach

Soils which have not been disturbed since 1951 have been shown to provide accurate inventories of some radioactive materials when normalized per unit area. This inventory includes ^{137}Cs deposited from atmospheric weapons testing (Loughran et al. 1982). The sampling locations chosen for this study (Table 2, Figure 15) were selected in a manner to help characterize the approximate 1,013 lakes within the Sawtooth Wilderness. Selected lakes were limited to the approximately 125 with official names to provide repeatability in sampling and assurance of the lake's permanence; e.g. the lake does not dry up in the summertime. Additional factors in selecting sampling locations included safe accessibility to the site, the dispersion of sampling sites throughout the wilderness, ice-cover, elevation, and "Leave No Trace" principles promoted by the National Forest Service. Even as late as July, the heavy snowfall from the previous winter prevented access to the southern and western parts of the Sawtooth Wilderness. This limited sampling to Blaine and Custer counties. Sampling was then modified to characterize the latitudinal dispersion of ^{137}Cs from the northernmost lakes to the southeast corner of the wilderness area. Selected sites were restricted to those with trail access to prevent environmental disruption as requested during the online and in-class "Leave No Trace" instructions completed on 3 and 6 July, respectively. Sampling was additionally limited to lakes above an elevation of 1,500 m to meet the alpine criteria and in order to collect the most undisturbed sediment cores. The following lakes were sampled following approval from the National Forest Service.

Table 2. Sampling Locations for ^{137}Cs in the Sawtooth Wilderness

Lake	Primary Outflow	Elevation	Location	County
Alice Lake	Pettit Lake Creek	2,622 m	43.9429°N 114.940853°W	Blaine
Bench Lake 1	Redfish Lake Creek	2,362 m	44.117031°N 114.950625°W	Custer
Hell Roaring Lake	Hell Roaring Creek	2,258 m	44.023822°N 114.936381°W	Custer
Little Sawtooth Lake	Iron Creek	2,570 m	44.180819°N 115.062421°W	Custer



Fig 15. Sampling Sites Within the Sawtooth Wilderness. Red-sample sites, Blue-lakes not being sampled

The sampling of four lakes made Idaho the ninth most-sampled state for radionuclide sediment concentrations since 1989, tied with Florida, Illinois, and New Jersey.

A Sand-Sludge-Sediment Probe soil-corer from Arts Machine Shop Inc. was used to take the sediment cores. The corer had a diameter of 3.18 cm and was capable of sampling to a 90-cm depth. This probe type came equipped with a core catcher tip to ensure full sample recovery within a 2.5-cm diameter poly liner insert (AMS 2016). The cores formed a compacted plug at the end of the corer which retained the sediment during withdrawal. The liners were replaceable after each sample, allowing multiple samples to be taken in a single trip. A complete list of equipment can be found in Appendix A.

Sample Collection

The pH of each lake was measured prior to sampling. Fifteen to twenty-two locations within each lake were sampled. Sampling locations were determined visually on site. All samples were taken at depths between 1 to 2 meters since the equipment was not suited for deep-water coring. Sampling was conducted away from lake inlets and outlets on relatively flat basins where possible. This decreased the potential impact of sediment focusing (Davis and Ford 1982). However, samples were taken as deep as possible with the given equipment where disturbance of the sediment would be least likely and where the bulk properties of the sediment would be more homogenous (Van Metre et al. 2004). Sampling was completed by manually pressing the soil corer into the sediment by hand or with the assistance of a small sledgehammer. The bottom of the core was capped as soon as it was pulled from the sediment bed to prevent sample loss during retrieval. Although similar lakes sampled within the 40°N to 50°N Latitude Band by various other investigations have recorded ^{137}Cs activity to depths of 40 cm (Heit and Miller 1987), the rocky bottoms characteristic of Idaho's alpine lakes prevented sampling below 25 cm. Cases in which sampling was limited to one side of the lake were also due to impenetrable rocky sediment. The average sampling depth achieved across 68 samples was limited to about 13 cm.

Repeat samples were completed at Hell Roaring Lake, taken within 1 m of each other at each sampling site, to determine the coefficient of variation among samples. Cores were kept upright, drained of excess water above the sediment, capped, and secured with parafilm to minimize the potential for disturbance during transport down the mountains. Specific sampling details for each lake can be found in Appendix B.

The sediment cores were kept in a vertical position and frozen within the poly-liner immediately upon return to Pocatello, ID. They were then sectioned into 1-cm segments using a PVC pipe cutter. The cutter was cleaned with a wet towel following each segmentation to prevent cross-contamination between samples. Error in depth was determined to be 0.1 cm, correlating with the thickness of the PVC pipe cutter. The core segments were oven-dried at 115°C for three hours and combined by depth strata to provide better measurement statistics. The combination was necessitated by the small corer diameter and low sediment density in order to gain enough mass to achieve the desired minimum detection concentration. The segments were manually homogenized, sieved to 2 mm, placed in pre-weighed 50 x 9-mm polystyrene petri dishes (Figure 16), and weighed to the nearest 0.01 g. Deeper strata were able to be split into multiple samples due to a higher sediment density in the bottommost portions of the cores, which added to the number of repeat samples.

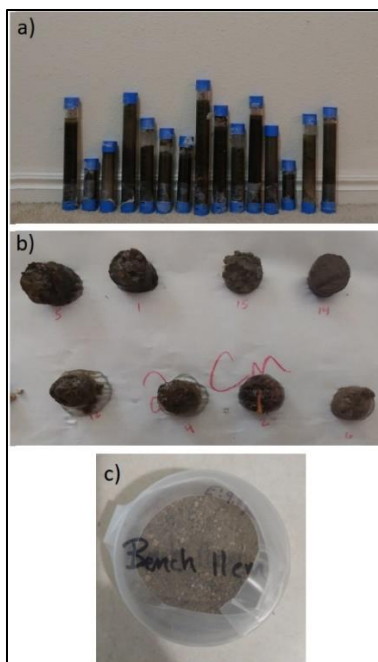


Fig 16. Sample Preparation a) poly liners trimmed to core depth and frozen b) cores segmented and oven-dried c) segments homogenized and sieved into analysis containers

Three background samples were collected in accordance with specifications from the Multi-Agency Radiation Survey and Site Investigation Manual (MARSSIM). The background's purpose was to provide a basis for comparison of ^{137}Cs levels with samples collected from the lakes (MARSSIM 2000b). The literature review indicated that ^{137}Cs from weapons testing was not found below 80 cm in soils surrounding alpine lakes. Therefore, the background samples were collected off-site at a depth of 92 cm where there was little chance of migration of the contaminant of concern. The soil at the background sampling site (42.906078°N, 112.432819°W) had similar physical characteristics as the soil being evaluated, as described in MARSSIM chapter 4 (MARSSIM 2000a). The background samples were then loaded into the same polystyrene petri dishes that the spike and lake samples would be analyzed in and measured on the HPGe detectors. No ^{137}Cs was detected in any of the background samples.

Sample Analysis

Analysis of each sample was performed in the Environmental Assessment Laboratory in the basement of the Physical Sciences building at Idaho State University. Samples were counted on coaxial HPGe detectors atop each detector's sample stand. Each detector was connected to an MCA with 8,192 channels (correlating the 661.6-keV photopeak of ^{137m}Ba to channel 2,712) and computer in accordance with Fig. 12. The MCAs were calibrated for efficiency and an energy range from 88 to 1,836 keV. Genie PROcount-2000 analysis software was used to determine the net count rate of ^{137}Cs and efficiency for each segment, allowing for the calculation of activity from eqn 4.

A Mixed Analyte Performance Evaluation Program (MAPEP) source with a known activity of ^{137}Cs (Appendix C) was used to create spiked soil samples. Three such spikes in the same geometry as the sediment samples were developed in order to ensure radioactive homogeneity within the MAPEP source and to determine the ^{137}Cs detection efficiency of each HPGe detector. The MAPEP spiked samples were counted with each detector for ten minutes and showed that Detector 4 (Princeton Gamma-Tech model IGC33, crystal diameter: 64 mm, crystal length: 38.5 mm, stand height: 2 cm) and Detector 7 (Canberra model GRI520, crystal diameter: 46.5 mm, crystal length: 39 mm, stand height: 1.5 cm) had the highest detection efficiencies for ^{137}Cs . The spiked sample analysis also determined that the range of sample densities of concern had no significant effect on counter efficiency. These two detectors were therefore used for all sample analyses. All three background and spiked samples were counted on Detector 4 and Detector 7 for 72,000 s. Efficiency for each detector was calculated using eqn 2. The percent efficiency for Detector 4 was calculated to be $1.89 \pm 5.6 \times 10^{-5}$, while the percent efficiency for Detector 7 was $0.98 \pm 4.0 \times 10^{-5}$. Measured activity values for the spikes and backgrounds were then averaged

and used to calculate L_D and MDC for each detector in accordance with eqns 7 and 8. An analysis time of 252,000 s was selected in order to minimize the MDC values for each detector within the time constraints of the laboratory. The resultant MDCs were $0.042 \pm 1.3 \times 10^{-4}$ Bq kg⁻¹ and $0.031 \pm 1.2 \times 10^{-4}$ Bq kg⁻¹ for Detectors 4 and 7, respectively, which were similar to those seen in the literature review studies.

All samples were counted atop the detector stands. Activity of ¹³⁷Cs was measured via the 661.6-keV gamma-energy line. The net emission rates were then corrected for sample geometry, detector efficiency, yield, and radioactive decay to the day of collection to calculate activity concentration (Bq g⁻¹) via eqn 4. Lake Alice and Bench Lake 1 were counted on Detector 7, while Little Sawtooth Lake and Hell Roaring Lake were counted on Detector 4. Repeat samples were counted on the same detector. Each segment of the lake's composite core sample was measured until the activity of ¹³⁷Cs was no longer detected. The maximum peak concentration of ¹³⁷Cs was assigned the year 1964. Any secondary peaks seen were assigned the year 1959, and the year in which the ¹³⁷Cs became detectable above background was assigned the year 1945 to correlate with the first year of a nuclear detonation per recommendation from Whicker et al. (1994). A linear regression plot of marker depth versus marker age was then created from the core data markers to estimate the mean sedimentation rate from the resulting slope.

Quality Assurance

Quality assurance for the ¹³⁷Cs analysis was provided by analyzing the MAPEP standard reference material, two environmental split samples, a repeat sample, and a blank sample with each batch of lake core samples. Median relative percent difference for ¹³⁷Cs for all reference material was 6.5% for Detector 4 and 5.2% for Detector 7. The median relative percent difference for ¹³⁷Cs in the reference material between the two detectors was 0.37%. Split

sediment samples analyzed had a median relative percent difference of 9.9%, while repeat samples had a median relative percent difference of 9.6. Daily checks were within 5.8% for Detector 4 and within 4.7% for Detector 7 throughout the duration of the study.

Chapter IV: Results

Cesium-137 Depth Profiles

The measured depth profiles in the scatter plots given below show ^{137}Cs concentrations plotted against depth. Depth markers represent the 1-cm segment sampled above the stated value; i.e. the 2-cm marker represents the soil sampled from a depth of 1 cm to 2 cm. Cesium-137 was detected above the L_C in all of the lakes. Three of the four lakes had ^{137}Cs depth distributions in sediment that resembled expected deposition patterns of weapons testing as a function of time. Numerical values are in Appendix F.

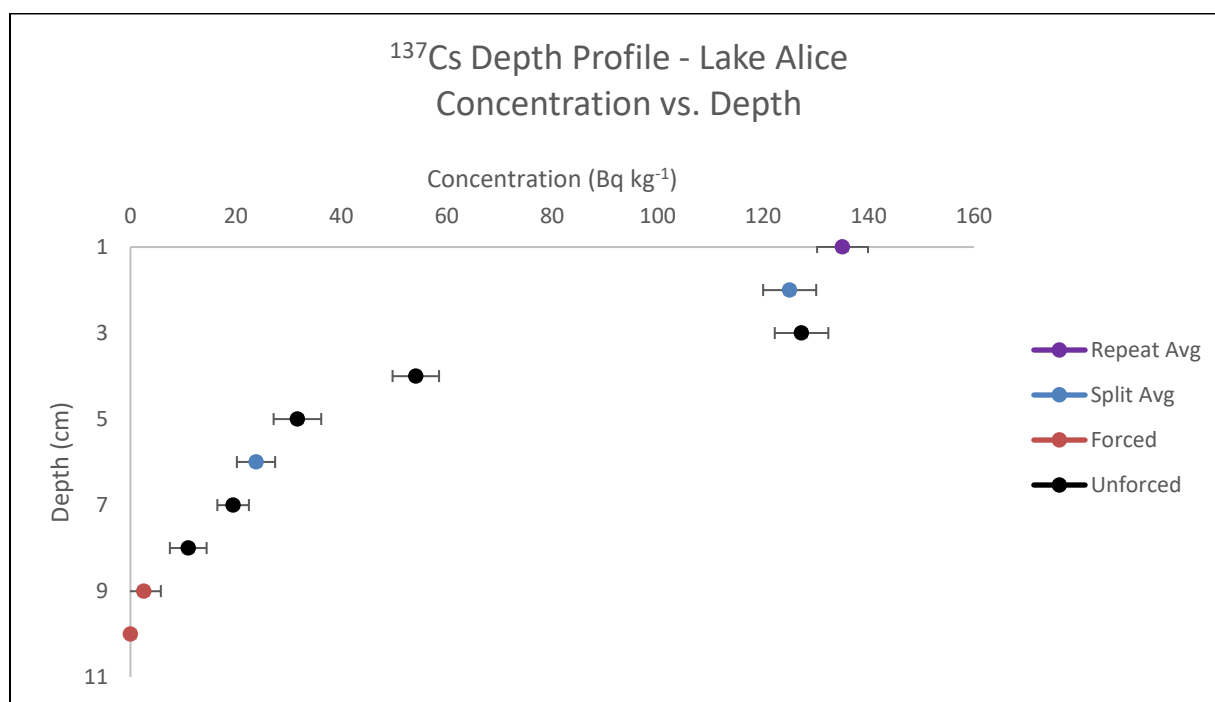


Fig 17. Lake Alice ^{137}Cs Depth Profile

Lake Alice was the southernmost lake sampled, situated at the highest altitude amongst the tested lakes. Because of the rapid inlets and outlets, samples were obtained from the northwest and southeast banks of the lake. Cores were collected at a water depth of 1 m. The sediment was composed of densely packed rock and sandy soil from the surrounding mountain slopes, requiring the assistance of a sledgehammer to attain the cores. The average sample weight was

7.26 g, equating to a sediment density of 410.9 kg m^{-3} . The maximum concentration of ^{137}Cs measured at Lake Alice was $135.1 \pm 4.82 \text{ Bq kg}^{-1}$ in the topmost centimeter of sediment. A second peak concentration of $127.3 \pm 5.08 \text{ Bq kg}^{-1}$ was measured at 3 cm (Figure 17). The deeper peak likely correlates to the year 1964. However, the presence of a single ^{137}Cs peak is an indicator of mixing or resuspension mechanisms (Heit and Miller 1987). Speculation consistent with the concepts published by Anderson et al. suggested that the combined effects of ^{137}Cs leaching, dispersion, and the postdepositional mixing of the sediment can be attributed to the large amount of runoff experienced from the previous winter's snowmelt affecting the shallow sampling depths (Anderson et al. 1987). Cesium-137 activity above background was detected to a depth of 8 cm. The estimated sedimentation rate for Lake Alice based on the identified dates is $0.10 \pm 0.03 \text{ cm y}^{-1}$ (Figure 21).

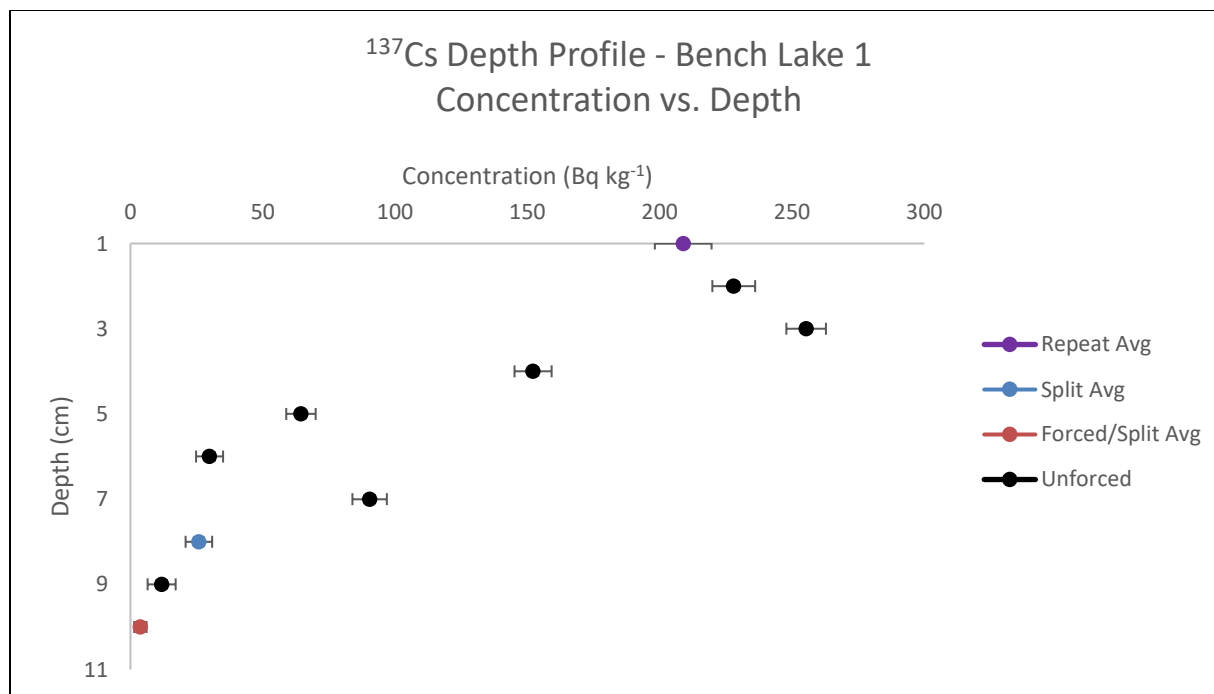


Fig 18. Bench Lake 1 ^{137}Cs Depth Profile

The sediment of Bench Lake 1 was mostly composed of organic plant matter, which left little medium available for analysis following the dehydration phase of sample preparation. The

average sample weight was 4.54 g, equating to a sediment density of 256.7 kg m^{-3} . A single low-flow inlet and outlet allowed cores to be collected around the whole perimeter at water depths between 1 and 2 m. The stagnant nature of the lake limited postdepositional mixing and dispersion, which allowed observation of peaks aligning to both 1959 and 1964. The largest ^{137}Cs concentration of $255.3 \pm 7.48 \text{ Bq kg}^{-1}$ was measured at a depth of 3 cm. The additional 1959 peak, with a ^{137}Cs concentration of $90.4 \pm 6.51 \text{ Bq kg}^{-1}$, was measured at a depth of 7 cm (Figure 18). Radioactivity above background was present to a depth of 9 cm. Bench Lake 1 was the bottommost lake in a five-chain series along Redfish Lake Creek. As such, it collected the ^{137}Cs runoff from the surrounding mountains and the leaching from the four lakes of higher elevation. Resultant ^{137}Cs concentrations were the highest measured among the lakes. The measured sedimentation rate was also the highest, averaging $0.12 \pm 0.05 \text{ cm y}^{-1}$ when compared to recognized fallout chronology.

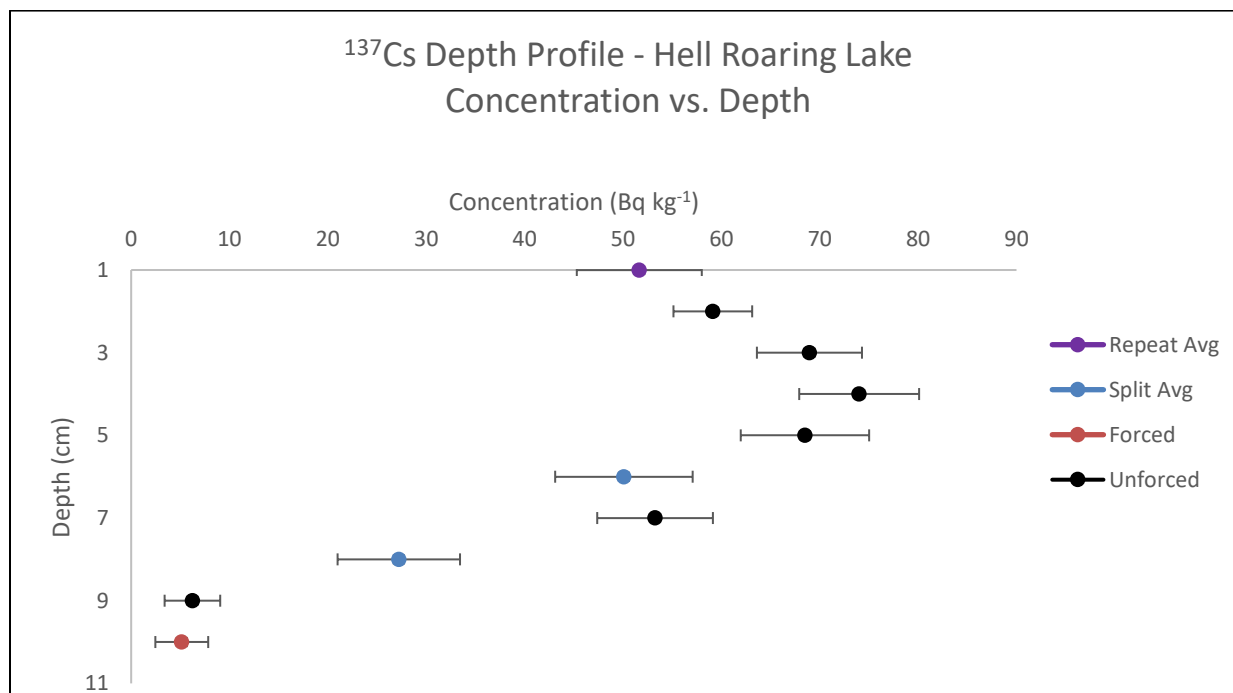


Fig 19. Hell Roaring Lake ^{137}Cs Depth Profile

The lower elevation of Hell Roaring Lake positioned it in a densely wooded area in an alpine basin (Leidecker 2011). The lake's placement in the canyon has left it vulnerable to avalanches, which have created a rocky lakebed coupled with toppled lodgepole pines. Sampling was limited to the northwest and southeast banks at depths between 1 and 2 m where corer penetration was possible amongst the debris. Samples were the least dense of the lakes as a result of sieving away pine fragments larger than 2 mm during the preparation phase. The average sample weight was 3.61 g, equating to a sediment density of 204.2 kg m^{-3} . The largest ^{137}Cs concentration peak was measured to be $74.0 \pm 6.09 \text{ Bq kg}^{-1}$ at 4 cm. A secondary peak at a depth of 7 cm had a concentration of $53.3 \pm 5.88 \text{ Bq kg}^{-1}$ (Figure 19). Cesium-137 activity above background was detected to a depth of 9 cm. The correlating sedimentation rate for Hell Roaring Lake based on the identified dates is $0.12 \pm 0.03 \text{ cm y}^{-1}$.

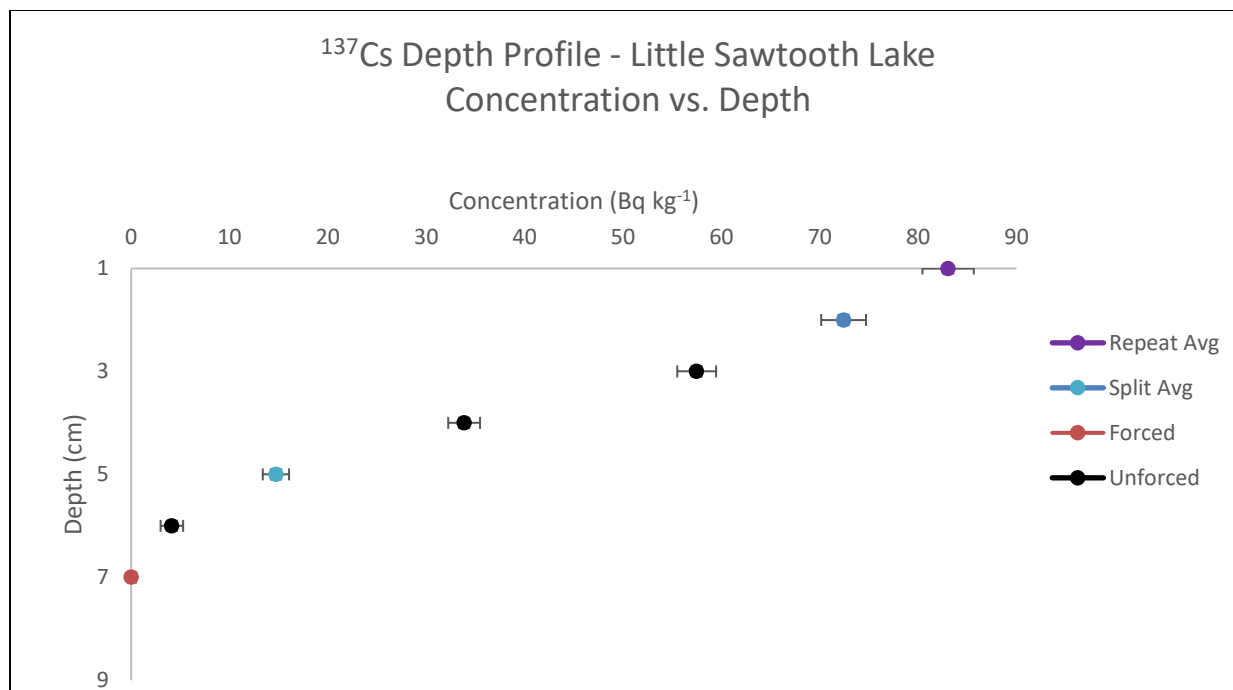


Fig 20. Little Sawtooth Lake ^{137}Cs Depth Profile

Little Sawtooth Lake was the northernmost lake sampled. The substrate was composed of densely packed soil as a result of runoff from the surrounding peaks. The resultant average

sample weight of 11.6 g equated to a substrate density of 656.2 kg m^{-3} ; the highest of all the sampled lakes. The banks of the lake were frozen at the time of sampling in late July, and the ice needed to be broken prior to sampling. Sampling was completed at a water depth of 1 m along the southern and eastern shores, which were trail accessible. The maximum concentration of ^{137}Cs measured at Little Sawtooth Lake was $83.0 \pm 2.61 \text{ Bq kg}^{-1}$ in the topmost centimeter of sediment (Figure 20). Radioactivity above background was measured to a depth of 6 cm. No peaks correlating with fallout chronology were discovered. The absence of peaks suggests mechanisms of flushing and resuspension of ^{137}Cs into the water column reduced the cesium concentration in the sediment though additional factors may also be responsible. Flushing occurs during periods of thaw, when atmospherically transported pollutants deposited onto the ice are released into the surface water and transported downstream prior to depositing into the sediment (Heit and Miller 1987). Sediment resuspension was likely caused by external disturbance, such as from excessive runoff turbulence following the 2016 winter or anthropogenic activities. The estimation of the sedimentation rate was limited by the presence of only two date markers (1945 at 6 cm and 2017 at 0 cm). However, these values correlate to a sedimentation rate of $0.08 \pm 0.29 \text{ cm y}^{-1}$.

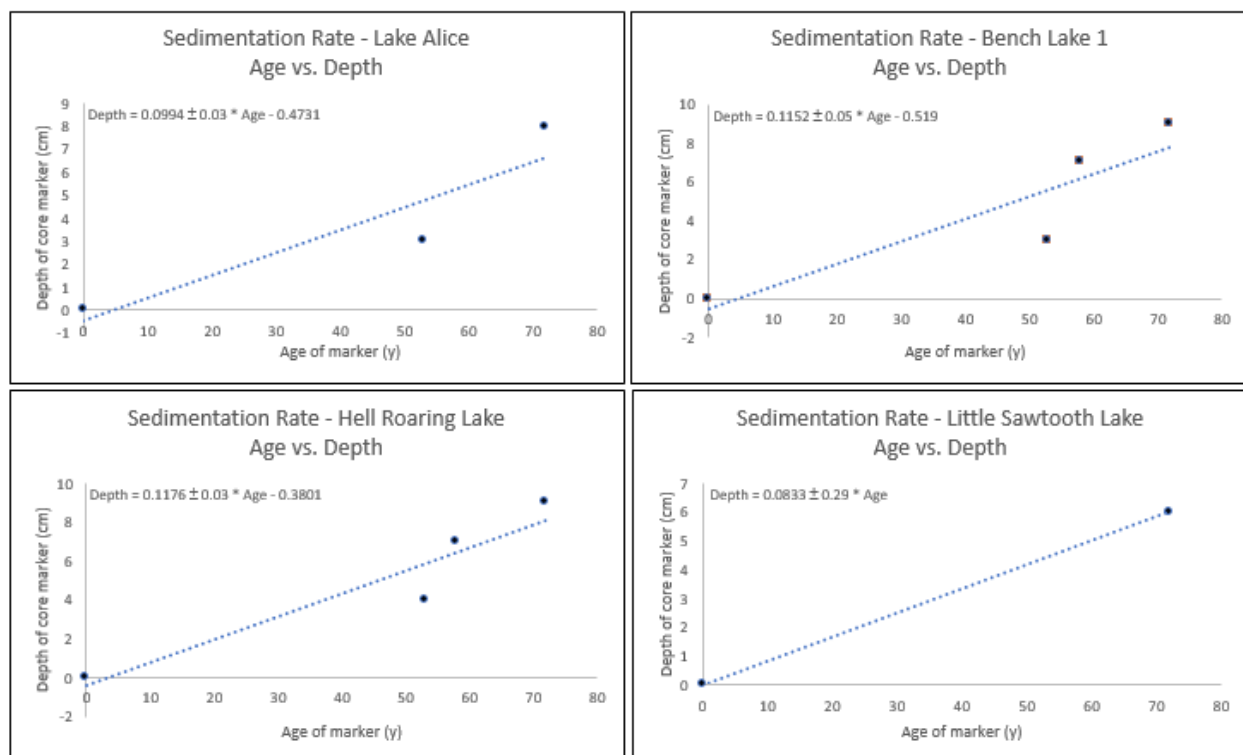


Fig 21. Sedimentation Rate Charts

It should be noted that dates assigned to ^{137}Cs concentrations vary among studies. This study follows the model proposed by Whicker et al. (1994), assigning dates of 1945, 1959 and 1964 to the appearance, secondary peak and primary peak, respectively. However, his study concluded that lakes with only a single measured peak should have a fallout date of 1962 assigned as an average between 1959 and 1964 (Whicker et al. 1994). Heit and Miller in 1987 suggested dates of 1951 for the first year of major weapons testing, 1958.5 for the secondary peak, and 1963 for the primary peak (Heit and Miller 1987). Riley Post in 2011 suggested 1964 for the primary peak and 1952 for the first appearance year, with secondary peaks in 1986 from the Chernobyl accident and 2011 from Fukushima (Post 2011). Application of these other dates to this study would slightly modify the estimated sedimentation rates.

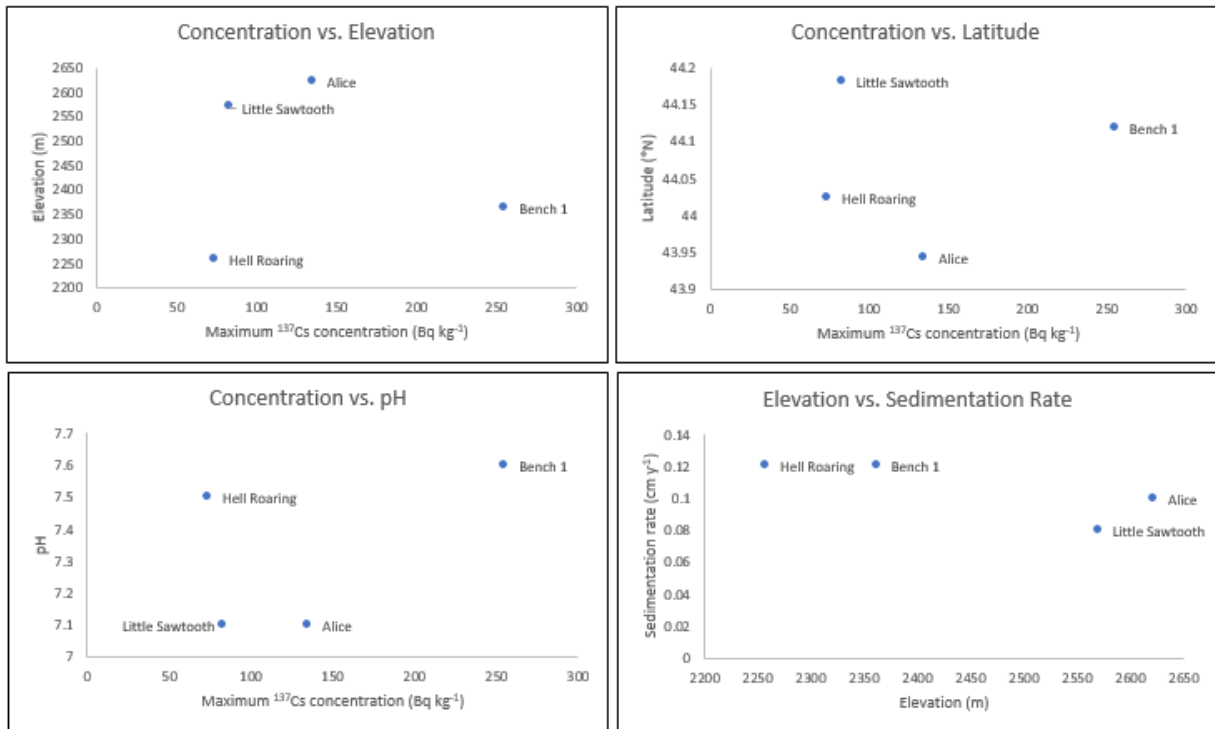


Fig 22. Deposition and Sedimentation Relationships to Elevation, Latitude and pH

By inspection, the scatter plots in Fig. 22 indicate no trends exist when maximum ¹³⁷Cs concentration measured is compared against lake elevation, geographical latitude, and pH. However, sedimentation rate tends to decrease with elevation gain.

This study quantified ^{137}Cs concentrations in the sediments of four lakes within Idaho's Sawtooth Wilderness. The maximum ^{137}Cs concentrations measured in each lake's sediment ranged from $74.0 \pm 6.09 \text{ Bq kg}^{-1}$ in Hell Roaring Lake to $255.3 \pm 7.48 \text{ Bq kg}^{-1}$ in Bench Lake 1. This range of ^{137}Cs concentrations was greater than the 95% L_C for all lakes as measured from the 661.6-keV $^{137\text{m}}\text{Ba}$ gamma-emission, equating to a z-score > 1.645 . The null hypothesis stating the samples would not contain measurable radioactivity above background was therefore rejected. Uncertainty was mainly attributed to sampling variations and the effects of spatial heterogeneity of the ^{137}Cs , with minor contribution from counting and laboratory error. Factors such as elevation, latitude and pH showed no correlation to total ^{137}Cs deposition. However, the data developed during this investigation suggested that characteristics such as geological location or lake flushing patterns are important factors in the total ^{137}Cs deposition observed. Positive radioactivity measurements in the lakes, both isolated and contiguous, appear to be consistent with observations made by Whicker et al. that demonstrate ^{137}Cs deposition in sediments is a combination of both direct deposition onto the lake and deposition on soils in the watershed which erode and wash into the lake as sediment (Whicker et al. 1994). Heit and Miller (1987) demonstrated that ^{137}Cs deposited directly is mobilized from the sediments by diffusion into the hypolimnion before being redeposited in areas of reduced current. Cesium-137 deposited on the snow, ice, and surrounding soils is released into the surface water during periods of thaw and runoff. Significant fractions are flushed from the lakes prior to being deposited in the sediment by the substantial water flow during these periods (Heit and Miller 1987). It is suspected that geological formations surrounding the lake and sediment flushing were the primary influences relating to maximum ^{137}Cs deposition. These factors were observed at Bench Lake 1, the bottommost impoundment in a five-chain series of contiguous lakes, having the highest ^{137}Cs

sediment concentration. Measured geochronological markers from fallout were used to estimate sedimentation rates for each lake. Mean sedimentation rate estimates ranged from 0.08 ± 0.29 cm y^{-1} in Little Sawtooth Lake to 0.12 ± 0.05 cm y^{-1} in Bench Lake 1. This is consistent with the observations of Whicker et al. who reported that sedimentation rates generally decreased with altitude gain as a result of reduced total runoff, erosion potential, and subsequent sedimentation in lower water bodies (Whicker et al. 1994).

Future Research Possibilities

Wilderness accessibility was the greatest limitation to this study. Multiple study plans were modified to accommodate access to lakes that were not isolated from rapid river crossings or washed out roads from the previous winter's runoff. The four lakes ultimately chosen were selected more so on accessibility than a statistical sampling plan. Performing this same study following a winter of lesser snowfall would grant access to southern and western lakes in the Sawtooth Wilderness, whose trailheads also grant access to the centermost locations.

Another limitation was the sampling equipment utilized in the study. The geographical locations of each of the lakes requires approximately ten miles of hiking round trip, and all equipment needed to be carried in by the researcher. Weight, financial considerations, and corer diameter were factors since the corer would need to be manually driven into the sediment. Selected coring equipment was not suited for deep-water sampling or large-diameter cores. Therefore, sediment at the deepest parts of the lakes was not collected, and analysis times were 252,000 s to accommodate the low sediment mass collected from the thin corer. Additionally, the corer geometry was challenged by the wide variety of sediment types present in the alpine lakes. The use of a larger corer diameter in future studies would significantly reduce analysis time and support sampling of a larger variety of sediments rich in rock and wood.

The use of larger teams would reduce the limit on the amount of measuring equipment that could be brought into the remote areas. The U.S. Geological Survey study from 1992-2001 had manpower capable of moving inflatable rafts to the alpine lakes to grant access to deep-water sediment (Van Metre et al. 2004). The use of other sensors that could provide measurements of flow and lake sediment load could provide insight into other mechanisms affecting the sedimentation rate of atmospherically transported pollutants. Heit and Miller in 1987 suggested that multiple mechanisms are responsible for ^{137}Cs sediment inventories, claiming binding-clay density, organic content, pH, dissolved oxygen, and flushing may all be possible factors (Heit and Miller 1987). Many studies substantiate these claims and could be verified with Idaho's alpine lakes. Clay content rich in silicates, vermiculites, and micas have been shown to preferentially adsorb ^{137}Cs (Francis and Brinkley 1976). The presence of organic ligands has been shown to affect the binding capacity of sediment, temporarily retaining fallout deposition radionuclides (Lehr and Kirchmann 1973). Pond sampling in Australia suggested acidic waters release ^{137}Cs from sediment (Longmore et al. 1983). Finally, studies of lakes with anoxic hypolimnions projected that the iron-manganese redox cycle may be responsible for increases in hypolimnetic concentrations of ^{137}Cs (Alberts et al. 1979).

The Bench five-lake system would be an ideal location to test for ^{137}Cs flushing in contiguous lakes. The highest lake (Bench Lake 5) would have a much lower ^{137}Cs inventory than Bench Lake 1 if flushing was present. Such results would confirm that atmospherically transported pollutants deposited onto the lakes or surrounding snow are released into the surface water and flushed from the lakes to areas of lower flow prior to deposition (Driscoll et al. 1987). It should be noted, however, that the two uppermost Bench Lakes are not trail accessible and sampling

should be conducted responsibly within the “Leave No Trace” principles promoted by the National Forest Service.

References

- Alberts JJ, Thilly LJ, Vigerstad TJ. Seasonal cycling of cesium-137 in a reservoir. *Science* 203: 649-651. 1979.
- Anderson RF, Schiff SL, Hesslein RH. Determining sediment accumulation and mixing rates using lead-210, cesium-137, and other tracers--Problems due to post-depositional mobility and coring artifacts. *Canadian Journal of Fisheries and Aquatic Sciences*, v. 44, 231-250. 1987.
- Arts Machine Shop, Inc. Sand sludge sediment probe. 2016. Available at <https://www.ams-samplers.com/hand-tooling/sludge-and-sediment-samplers/sludge-and-sediment-samplers/sand-sludge-sediment-probe.html>. Accessed 30 August 2017.
- Berkeley University. How we calculate minimum detectable activity. 2014. Available at <https://radwatch.berkeley.edu/MDACalculation>. Accessed 19 February 2017.
- Brey R. Semiconductor detectors. In: HPHY 4416/5516: Introduction to nuclear measurements. Pocatello, ID: Idaho State University; 28 March 2017. Lecture.
- Brey R, Claver K. Gamma ray spectroscopy. In: HPHY 4416/5516: Introduction to nuclear measurements; 2017: 87-95.
- Comans RNJ, Haller M, de Preter P. Sorption of cesium on illite: nonequilibrium behavior and reversibility. *Geochimica et Cosmochimica Acta*, 55, 433-440. 1991.
- Currie LA. Limits for qualitative detection and quantitative determination. National Bureau of Standards. ID: 20234. 1968: 1-7.
- Davis MB, Ford MS. Sediment focusing in Mirror Lake, New Hampshire. *Limnol. Oceanography* 27:137-150. 1982.
- Dricoll CT, Yatsko CP, Unangst FJ. Longitudinal and temporal trends in the water chemistry of the North Branch of the Moose River. *Biogeochemistry* 3: 37-61. 1987.
- Durham RW, Joshi SR. Radioactive dating of sediment cores from four contiguous lakes in Saskatchewan, Canada. *Science Total Environ.* 15:65-71. 1980.
- Eisenbud M, Gesell T. Environmental radioactivity from natural, industrial, and military sources fourth edition. Academic Press. 1997; 306.
- Environmental Measurements Laboratory. Appendix to the Environmental Measurements Laboratory Environmental Quarterly. pp. A1-A400. U.S.E.R.D.A. Report EML-3210, New York, NY 10014. 1977.

Ewert D, Sara E. "Peak park politics: the struggle over the Sawtooths, from Borah to Church". *The Pacific Northwest Quarterly*. Seattle, WA: University of Washington. 91 (3): 138–149. ISSN 0030-8803. JSTOR 40492581. 2000.

Fesenko S, Fesenko J, Sanzharova N, Karpenko E, Titov I. Radionuclide transfer to freshwater biota species: review of Russian language studies. *Journal of Environmental Radioactivity*, 102, 8–25. 2011.

Francis CW, Brinkley FS. Preferential adsorption of ^{137}Cs in contaminated freshwater sediment. *Nature* 260: 511-513. 1976.

Galloway JN, Likens GE. Atmospheric enhancement of metal deposition in Adirondack Lake sediments. *Limnol. Oceanography* 24:427. 1979.

Heit M, Tan YL, Klusek CS, Volchok HL, Burke JC. The origin and deposition history of trace elements and polynuclear aromatic hydrocarbons in two remote lakes in the Adirondack acid rain region. pp. 1-75 to 1-127. U.S.D.O.E. Report EML-381, New York, NY 10014. 1980.

Heit M, Tan YL, Miller KM, Quari J, Marnetti C, Silvestri S. The sediment chronology and polycyclic aromatic hydrocarbons concentrations and fluxes in Cayuga Lake, NY sediments. U.S. D.O.E. Report EML-451. 1986: 1-53.

Heit M, Miller KM. Cesium-137 sediment depth profiles and inventories in Adirondack Lake sediments. *Biogeochemistry* 3:242-265. Springer Publishing; 1987.

Jaakkola T, Tolonen K, Huttunen P, Leskinen S. The use of fallout ^{137}Cs and $^{239+240}\text{Pu}$ for dating of lake sediments. *Hydrobiologia* 103:15. 1983.

Knoll G. Minimum detectable amount (MDA). In: *Radiation detection and measurement third edition*. John Wiley & Sons, Inc. 2000; 96-98.

Knoll G. Semiconductor diode detectors. In: *Radiation detection and measurement third edition*. John Wiley & Sons, Inc. 2000; 366-374.

Konzen K. Lesson 10: Semi-conductor detectors. In: *HPHY 4432/5532 Radiation physics II*. Pocatello, ID: Idaho State University; 2017: 1-65.

Krey PW, Hardy EP, Heit M. Nevada Test Site fallout in the area of Enterprise, Utah. U.S. D.O.E. Report, EML-372, New York, NY 10014. 1980.

Krey PW, Beck HL. The distribution throughout Utah of ^{137}Cs and $^{239+240}\text{Pu}$ from Nevada Test Site detonations. U.S. D.O.E. Report, EML-400, New York, NY 10014. 1981.

Krey PW, Heit M, Miller KM. Radioactive fallout reconstruction from contemporary measurements of reservoir sediments. *Health Phys.* 59: 541-54. 1990.

Lehr JJ, Kirchmann R. The contamination by radiostrontium and radiocesium of grassland in relation to the age of deposition and to the organic matter in the soil. *International Journal Environmental Studies* 5: 99-104. 1973.

Leidecker M. Hell Roaring Lake. Idaho River Publications. 2011. Available at <https://www.outdoorproject.com/adventures/idaho/hikes/hell-roaring-lake>. Accessed 21 Jan 2018.

Longmore ME, O'Leary BM, Rose CW. Caesium-137 profiles in the sediments of a partial-meromictic lake on Great Sandy Island, Queensland, Australia. *Hydrobiologia* 103: 21-27. 1983.

Loughran RJ, Campbell BL, Elliott GL. The identification and quantification of sediment sources using ^{137}Cs . In: *Recent developments in the explanation and predictions of erosion and sediment yield*. IAHS Publication No. 137. 1982. 361-369.

Martin J. Semiconducting detectors. In: *Physics for radiation protection: third, completely updated edition*. 2013; 494-495.

Martin J. *Physics for radiation protection third, completely updated edition*. Wiley VCH. 2013; 633-655.

Miller KM, Heit M. A time resolution methodology for assessing the quality of lake sediment cores that are dated by ^{137}Cs . *Limnology and Oceanography*. 1986.

Multi-Agency Radiation Survey and Site Investigation Manual. Revision 1. 4.5: Select background reference areas. In: *Chapter 4: preliminary survey considerations*. 2000. 13-14.

Multi-Agency Radiation Survey and Site Investigation Manual. Revision 1. 7.2: Data quality objectives. In: *Chapter 7: sampling and preparation for laboratory measurements*. 2000. 1-7.

National Nuclear Data Center. Chart of nuclides. 2017. Available at <http://www.nndc.bnl.gov/chart/reCenter.jsp?z=79&n=120>. Accessed 6 Jan 2018.

Nicholson KW, Branson JR, Giess P. Field measurements of the below-cloud scavenging of particulate material. *Atmospheric Environment*, 25A, 771-777. 1991.

Osborn J. "Creating the Sawtooth National Recreation Area, Protecting Wilderness". 1979. Archived from the original on February 12, 2013.

Pennington W, Cambray rs, Eakins JD, Harkness DD. Radionuclide dating of the recent sediments of Blelham Tarn. *Freshwater Biol.* 6:317-331. 1976.

Post RA. Determining lake sedimentation rates using radionuclide tracers. University of Iowa. Thesis. 1-79; 2011.

Poudel D. Prelab 9: High resolution gamma spectroscopy. Pocatello, ID: Idaho State University; 2015. Video. Available at: http://media.itrc.isu.edu/videos/?v=distance/201520/hphy4416_5516a/hphy4416_5516a_0330.flv&q=.dv. Accessed 27 March 2017.

Poudel D. Prelab 5: Proportional counter characterization. Pocatello, ID: Idaho State University; 2015. Video. Available at: http://media.itrc.isu.edu/videos/?v=distance/201520/hphy4416_5516a/hphy4416_5516a_0209.flv&q=.dv. Accessed 1 February 2017.

Poudel D. Prelab 6: Proportional counter environmental sampling. Pocatello, ID: Idaho State University; 2015. Video. Available at: http://media.itrc.isu.edu/videos/?v=distance/201520/hphy4416_5516a/hphy4416_5516a_0211.flv&q=.dv. Accessed 8 February 2017.

Robbins JR, Edgington DN. Determination of recent sedimentation rates in Lake Michigan using ^{210}Pb and ^{137}Cs . *Geochim. Cosmochim. Acta* 39:285-304. 1975.

Robbins JA, Lindner G, Pfeiffer W, Kleiner J, Stabel HH, Frenzel P. Epilimnetic scavenging and fate of Chernobyl radionuclides in Lake Constance. *Geochimica et Cosmochimica Acta*, 56, 2339–2361. 1992.

Saxén R, Ilus E. Transfer and behaviour of ^{137}Cs in two Finnish lakes and their catchments. *The Science of the Total Environment*, 394, 349–360. 2008.

Smith S. Determining sample size: how to ensure you get the correct sample size. 2013. Available at <https://www.qualtrics.com/blog/determining-sample-size/>. Accessed 10 May 2017.

Sparmacher H, Fulber K, Bonka H. Below-cloud scavenging of aerosol Particles: particle-bound radionuclides - experimental. *Atmospheric Environment*, 27A, 605-618. 1993.

Taylor JR. An introduction to error analysis: the study of uncertainties in physical measurements. University Science Books. 1997.

U.S. Forest Service Sawtooth National Forest (Map) (1998 ed.). Sawtooth National Forest.

Ulsh B, Rademacher S, Whicker FW. Variations of ^{137}Cs depositions and soil concentrations between alpine and montane soils in northern Colorado. *JER* 47: 57-70. 2000.

Van Metre P, Wilson J, Fuller C, Callender E, Mahler B. Collection, analysis, and age-dating of sediment cores from 56 U.S. lakes and reservoirs sampled by the U.S. Geological Survey, 1992-2001. *Scientific Investigations Report 2004-5184*: 1-187. 2004.

Western Michigan University. t-based confidence interval for the mean. 2003. Available at <http://www.stat.wmich.edu/s216/book/node79.html>. Accessed 19 February 2017.

Whicker FW, Pinder JE, Bowling JW, Alberts JJ, Brisbin IL. Distribution of long-lived radionuclides in an abandoned reactor cooling reservoir. *Ecol. Monogr.* 60(4): 471-96. 1990.

Whicker JJ, Whicker FW, Jacobi S. ^{127}Cs sediments of Utah lakes and reservoirs: effects of elevation, sedimentation rate and fallout history. JER 23: 265-283. 1994.

Appendix A
List of Materials

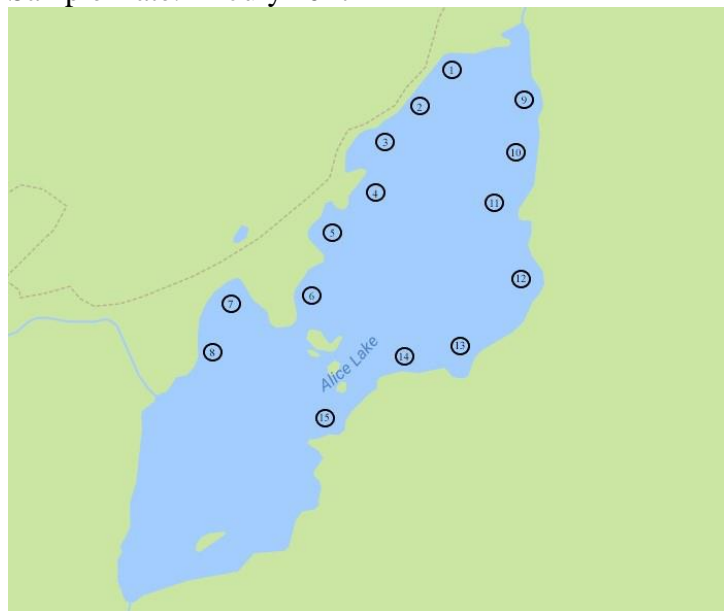
- Arts Machine Shop 1-1/4" x 36" replaceable tip sand probe (Part # 424.39)
- Arts Machine Shop 1" x 37-3/4" plastic liner (Part # 425.05)
- Arts Machine Shop 1" plastic end cap (Part # 425.18)
- Bayonet Neill-Concelman (BNC) cable
- BrassCraft 2-1/2" capacity ratcheting PVC pipe cutter (Part # T439)
- Canberra dewar, model GR1520
- Canberra Genie-2000 PROcount-2000 software, v1.2
- Canberra HPGe coax GR1520 detector (S/N 5902512, Det 07)
 - Complete details in Appendix E
 - Canberra 2002CSL RC preamplifier
 - Canberra 7500SL cryostat
 - Canberra ICB9645 high voltage power supply (4,000 V, positive polarity)
 - Canberra ICB9615 spectroscopy amplifier
 - Coarse gain - 100
 - Negative input polarity
 - Positive inh. polarity
 - Shaping time: amp 4 μ s
 - BLR mode: sym
 - Pole 0: 2926
 - Pur: on
 - Canberra ICB9633 analog-to-digital converter
 - Conversion gain: 8,192
 - Background circuitry: coinc.
 - Process Hazard Analysis mode
 - Offset: 0
 - LLD: 1.66%
 - ULD: 110%
- Canberra Nuclear Instrumentation Module (NIM) bin, model 2100
- Denver Instrument APX-1502 scale, d=0.01 g, cal: 3/10/2017 (I.D. A12982011)
- Falcon 50 x 9 mm sterile polystyrene petri dish (Part # BD 351006)
- Gilson Company compliance test sieve, 2.0 mm (S/N 172326766)
- Jellas pocket size pH meter, d=0.1 resolution, cal: 8 Jul 2017 (Part # JLPH01)
- Norco liquid nitrogen
- Ortec NIM fan, model M127/N
- Parafilm
- Princeton Gamma-Tech dewar, RG-11AC (S/N 2972)
- Princeton Gamma-Tech HPGe coax IGC33 detector (S/N 932, Det 04)
 - Complete details in Appendix E
 - Princeton Gamma-Tech RG-11A/C preamplifier
 - Princeton Gamma-Tech NPR/8 cryostat
 - Canberra 3105 high voltage power supply (3,500 V, positive polarity)

- Canberra 2025 spectroscopy amplifier
 - Coarse gain - 100
 - Negative input polarity
 - Shaping time: amp 4 μ s
 - Norm restorer threshold
 - Asym restorer mode
 - Pur: on
- ND579 analog-to-digital converter
 - Conversion gain: 8,000
 - Background circuitry: off
 - Process Hazard Analysis mode
- Radiological and Environmental Sciences Laboratory MAPEP (I.D. 16-MaS35)
 - Complete details in Appendix C
- Safe for High Voltage (SHV) cable
- Universal Serial Bus (USB) cable

Appendix B
Sample Maps

Table 4: Specifics of Alice Lake Sampling

Sample Date: 11 July 2017



Sample	Time
1	14:40
2	14:45
3	14:51
4	14:55
5	15:03
6	15:20
7	15:26
8	15:32
9	15:51
10	15:55
11	15:58
12	16:03
13	16:16
14	16:20
15	16:24

Table 5: Specifics of Bench Lake 1 Sampling

Sample Date: 2 August 2017



Sample	Time
1	10:59
2	11:05
3	11:09
4	11:16
5	11:20
6	11:26
7	11:44
8	11:49
9	12:04
10	12:06
11	12:10
12	12:22
13	12:24
14	12:27
15	12:30

Table 6: Specifics of Hell Roaring Lake Sampling

Sample Date: 7 August 2017



Sample	Time	Repeat Sample	Time
1	11:19	1	11:21
2	11:25	2	11:29
3	12:03	3	12:07
4	12:09	4	12:12
5	12:15	5	12:17
6	12:22	6	12:23
7	13:03	7	13:07
8	13:12	8	13:14
9	13:19	9	13:23
10	13:25	10	13:34
11	13:40	11	13:42

Table 7: Specifics of Little Sawtooth Lake Sampling

Sample Date: 25 July 2017



Sample	Time
1	11:54
2	11:57
3	11:59
4	12:03
5	12:06
6	12:09
7	12:11
8	12:16
9	12:20
10	12:24
11	12:27
12	12:28
13	12:31
14	12:34
15	12:37
16	12:40

Appendix C
MAPEP Data

Table 8. Mixed Analyte Performance Evaluation Program Soil Source (8/1/2016)

Radionuclide	Activity (Bq kg ⁻¹)	Error (Bq kg ⁻¹)	MAPEP activity (Bq kg ⁻¹)	Relative difference
⁴⁰ K	606.33	39.52	588	-3.12%
⁵⁴ Mn	1.54	0.98	FP	
⁵⁷ Co	1203.50	66.65	1190	-1.13%
⁶⁰ Co	894.99	44.73	851	-5.17%
⁶⁵ Zn	757.53	41.73	695	-9.00%
¹³⁴ Cs	-5.80	0.78		
¹³⁷ Cs	1099.65	61.15	1067	-3.06%

Appendix D Sawtooth National Recreation Area Project Approval

	United States Department of Agriculture	Forest Service	Sawtooth National Forest Sawtooth National Recreation Area	5 North Fork Canyon Road KetchumID83340 208-727-5000
---	---	-------------------	---	--

File Code: 2710
Date: July 5, 2017

Benjamin Bishop, Capt. USAF, BSC
 Health Physics Department
 Idaho State University
 921 S. 8th Ave - Mail Stop 8060
 Pocatello, ID 83209-8060

Dear Captain Bishop,

We are in receipt of your request to conduct lake-core sampling research in the Sawtooth National Recreation Area (NRA) at locations inside the Sawtooth Wilderness boundary. Based on our review of your written proposal and on follow-up discussions with our special uses administrator, we have determined that the proposed research activity will have only nominal effects on National Forest System lands, resources and programs. It is therefore not necessary to establish terms and conditions for your proposed activities through a special use authorization, (permit) in order to protect Forest System aquatic or lake bed resources or to avoid conflict with NRA programs, operations or resources. I conclude that a special use permit will not be required. This Letter constitutes my authorization.

We ask that you adhere closely to the plans and details provided, for your research and other activities, and that you abide by "leave no trace" principles as well as all relevant Sawtooth NRA regulations, orders and guidance, as you conduct your research and travel inside wilderness boundaries.

When operating on Sawtooth NRA lands please carry a copy of this letter in the unlikely event that your activities are questioned. Please contact Special Uses Administrator Art Fisher at (208) 727-5008, for any follow-up questions.

Good luck with your study. Please share any pertinent findings with us. Thank you for your responsiveness and co-operation in defining this activity.

Sincerely,


 Kirk Flannigan
 Area Ranger

Cc: Art Fisher, Special Uses Administrator



Caring for the Land and Serving People



Fig 23. Sawtooth National Forest Special Use Permit

Appendix E High Purity Germanium Detector Specifications

 PRINCETON GAMMA-TECH										
HPGe Coax Detector Final Test Record										
	Model Number	Serial Number								
Detector	IGC33	932								
Preamplifier	RG-11A/C	2972								
Cryostat	NPR/E									
Crystal Polarity	P TYPE	Endcap Material	Aluminum							
Crystal Diameter	64mm	Window Material	Aluminum							
Crystal Length	38.5mm	Window Thickness	1mm							
Core Diameter	10mm	Dead-layer Thickness	<1mm							
Core Length	27mm	Active Area	N/A							
Active Volume	115cm ³	Crystal to Window distance	5mm							
Detector Bias and Polarity	+ 3500V	Dewar Capacity	30L							
Preamp Output Polarity	Negative	Recommended Refill Time	12days							
Feedback Voltage at Operating Bias	-0.55	Cooling Period before Operation	8hrs							
		Operating Temperature	N/A							
HV	0	100	500	1000	1500	2000	2500	3000	3500	4000
TP Voltage	-0.49	-0.55	-0.55	-0.55	-0.55	-0.55	-0.55	-0.55	-0.55	-0.55
Noise (mV)	800	120	90	70	45	24	14	10	10	
Performance:		Guaranteed	Measured							
FWHM @ 1332 keV		2.6keV	1.71keV							
FWTM @ 1332keV		4.80keV	3.14keV							
FWHM @ 122 keV		N/A	.647keV							
FWHM @ 5.9 keV		N/A	N/A							
Relative Efficiency at 1332 keV		29.7%	31.6%							
Peak-to-Compton @ 1332 keV		51/1	60.7/1							
Associated Sales Order #	6872									
Associated Crystal File #	IGGY 425									
Test Equipment Conditions:										
Equipment	Model	S/N								
Amp/ADC	8016	110007								
HV	8016	110007								
DVM	22-181A	10A4								
Oscilloscope	OS5020	80603072								
Count Rate	1000cps									
Shaping Time	4us									
Tested by 		Date: 02-01-06								

Fig 24. Detector 04 Specifications

Table 9. Detector 04 Specifications

Avg. dead time (s)	Efficiency (%)	L _c (counts kg ⁻¹)	L _D (counts kg ⁻¹)	MDC (Bq kg ⁻¹)	662 keV error (keV)	1332 keV error (keV)	Avg. 662 keV net peak activity (counts)	Avg. 1332 keV full-width half max (keV)
89.7 ± 2.7	1.89 ± 5.6x10 ⁻⁵	83.6 ± 9.14	170 ± 108	0.042 ± 1.3x10 ⁻⁴	± 0.5	± 0.5	36,980 ± 1,110	1.85 ± 0.11

The dead time was the average value recorded across all samples. Efficiency, L_c, L_D, and MDC were calculated with eqns 3, 6, 7, and 8. The last four columns were a reflection of the detector's daily quality checks.

CANBERRA

DETECTOR SPECIFICATION AND PERFORMANCE DATA Rev. 6/13/99

Specifications

DETECTOR MODEL GR1520 SERIAL NUMBER 5902512
 CRYOSTAT MODEL 7500SL PREAMPLIFIER MODEL 2002CSL

The purchase specifications, and therefore the warranted performance, of this detector are as follows:
 (Electric cooling may degrade performance by as much as 10%.)

Active Volume _____ cc Relative Efficiency _____ %
 Resolution _____ keV (FWHM) at 1.33 MeV
 _____ keV (FWTM) at 1.33 MeV
 _____ keV (FWHM) at _____
 _____ keV (FWTM) at _____

Peak/Compton _____ :1 Cryostat well diameter _____ mm Cryostat well depth _____ mm
 Cryostat description (if special) 3.0" Ø End Cap

Physical Characteristics

Geometry Reverse Electrode Closed-end coaxial
 Diameter 46.5 mm Active Volume _____ cc
 Length 39 mm Well Depth _____ mm
 Distance from window 5 mm Well Diameter _____ mm

Electrical Characteristics

Depletion voltage -2500 V dc
 Recommended bias voltage -3000 V dc
 Test point voltage at recommended bias -2.15 V dc (RC preamp only)
 Reset interval at recommended bias _____ sec. (Reset preamp only)
 Capacitance at recommended bias -20 pF

Resolution and Efficiency

With amp time constant of 4 microseconds

Isotope	⁵⁷ Co	⁶⁰ Co		¹³⁷ Cs
Energy (keV)	122	1332		22.84
FWHM (keV)	0.90	1.81		
FWTM (keV)	1.66	3.32		
Peak/Compton		44.6:1		
Rel. Efficiency %		15.7		23.2:1

Cool Down Time 4 hours. Cryostat Liquid Nitrogen Consumption Rate <1.8 Liters per Day.

Tested by: [Signature] Date: 02/08/08
 Approved by: [Signature] Date: 02/08/08

BB Research Parkway, Norwalk, CT USA 06855 • Tel. 203-235-2325/Fax. 203-630-3423

Fig 25. Detector 07 Specifications

Table 10. Detector 07 Specifications

Avg dead time (s)	Efficiency (%)	L _C (counts kg ⁻¹)	L _D (counts kg ⁻¹)	MDC (Bq kg ⁻¹)	661.6 keV error (keV)	1332 keV error (keV)	Avg. 661.6 keV net peak activity (counts)	Avg. 1332 keV full-width half max (keV)
206.9 ± 31.2	0.98 ± 4.0x10 ⁻⁵	30.8 ± 5.55	64.2 ± 108	0.031 ± 1.2x10 ⁻⁴	± 0.5	± 0.5	42,162 ± 1,265	1.85 ± 0.09

The dead time was the average value recorded across all samples. Efficiency, L_C, L_D, and MDC were calculated with eqns 3, 6, 7, and 8. The last four columns were a reflection of the detector's daily quality checks.

Appendix F
¹³⁷Cs Deposition Numerical Sample Results

Table 11: ¹³⁷Cs Concentration Numerical Sample Results

Lake	Depth (± 0.1 cm)	Concentration (Bq kg ⁻¹)	Error (Bq kg ⁻¹)
Alice	1	135.064	4.823
	2	125.037	5.033
	3	127.288	5.082
	4	54.123	4.409
	5	31.669	4.515
	6	23.814	3.631
	7	19.471	2.993
	8	10.961	3.482
	9	2.547	3.218
	10	0.000	0.000
Bench Lake 1	1	208.872	10.716
	2	227.974	8.079
	3	255.327	7.484
	4	152.138	7.011
	5	64.428	5.563
	6	29.901	5.102
	7	90.381	6.509
	8	25.852	5.019
	9	11.777	5.296
	10	3.759	2.322
Hell Roaring Lake	1	51.654	6.354
	2	59.129	4.002
	3	68.950	5.341
	4	74.007	6.094
	5	68.494	6.526
	6	50.091	6.988
	7	53.257	5.880
	8	27.208	6.223
	9	6.226	2.825
	10	5.146	2.686
Little Sawtooth Lake	1	83.049	2.609
	2	72.424	2.277
	3	57.490	1.974
	4	33.848	1.617
	5	14.715	1.336
	6	4.138	1.147
	7	0.000	0.000